Journal of Medicinal Chemistry

pubs.acs.org/jmc

Article

Self-Adjuvanting Lipoprotein Conjugate αGalCer-RBD Induces Potent Immunity against SARS-CoV-2 and its Variants of Concern

Jian Wang,[‖] Yu Wen,[‖] Shi-Hao Zhou,[‖] Hai-Wei Zhang, Xiao-Qian Peng, Ru-Yan Zhang, Xu-Guang Yin, Hong Qiu, Rui Gong,* Guang-Fu Yang,* and Jun Guo*

Cite This: https://doi.org/10.1021/acs.jmedchem.1c02000

Read Online

ACCESS | Metrics & More | Article Recommendations | Supporting Information

ABSTRACT: Safe and effective vaccines against severe acute respiratory syndrome coronavirus 2 (SARS-CoV-2) and its variants are the best approach to successfully combat the COVID-19 pandemic. The receptor-binding domain (RBD) of the viral spike protein is a major target to develop candidate vaccines. α-Galactosylceramide (αGalCer), a potent invariant natural killer T cell (iNKT) agonist, was site-specifically conjugated to the *N*-terminus of the RBD to form an adjuvant−protein conjugate, which was anchored on the liposome surface. This is the first time that an iNKT cell agonist was conjugated to the protein antigen. Compared to the unconjugated RBD/αGalCer mixture, the αGalCer-RBD conjugate induced significantly stronger humoral and cellular responses. The conjugate vaccine also showed effective cross-neutralization to all variants of concern (B.1.1.7/alpha, B.1.351/beta, P.1/gamma, B.1.617.2/delta, and B.1.1.529/omicron). These results suggest that the self-adjuvanting αGalCer-RBD has great potential to be an effective COVID-19 vaccine candidate, and this strategy might be useful for designing various subunit vaccines.

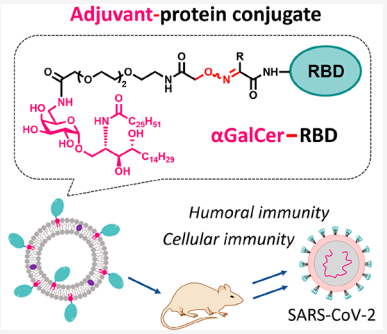

INTRODUCTION

The coronavirus disease 2019 (COVID-19) pandemic, caused by the severe acute respiratory syndrome coronavirus 2 (SARS-CoV-2), has severely affected public health and economic stability that led to social issues worldwide. As the emerging variants led to a mounting death toll, safe and effective vaccines were still the best manner to combat this global pandemic.

Since the COVID-19 outbreak, vaccine candidates against SARS-CoV-2 have emerged at an unprecedented scale and speed worldwide. In general, candidate vaccines are divided into six categories, including inactivated virus, live attenuated virus, recombinant viral vectors, protein subunits, virus-like particles, and nucleic acid-based candidates.[1] Although some advanced candidates have moved into clinical trial stages and have been granted licences,[2] uncertainties still remain due to the rapid spread of mutated SARS-CoV-2. Therefore, it is necessary to develop diverse platforms and strategies for preparing successful COVID-19 vaccines.

The spike (S) protein plays a pivotal role in binding to the angiotensin-converting enzyme 2 (ACE2) receptor on host cells via its receptor-binding domain (RBD),[3,4] which is the major target for protein subunit vaccines against COVID-19.[5−8] These vaccines are designed to induce immune responses toward specific epitopes (B and T cell epitopes) on the S protein, particularly on the RBD, thereby averting eosinophilic immunopathology or antibody-dependent enhancement (ADE) of the disease.[9] In addition, subunit vaccines are relatively safe and easily manufactured compared with traditional vaccines based on whole virus. Some commonly used chemicals to inactivate viruses are potentially carcinogenic such as β-propiolactone, which inactivate viruses at both the protein and nucleic acid levels, and thus may lead to destruction of the crucial antigenic protein structures.[10] However, the major drawback of protein subunit vaccines is their weak immunogenicity; thus, an adjuvant serving as a "danger signal" is often utilized in subunit vaccines to elicit robust humoral and cellular immunity.[11−13]

Among the subunit vaccine candidates against COVID-19, several adjuvants, including aluminum,[8,14] STING agonist cyclic di-GMP (CDG),[15] toll-like receptor (TLR) agonists such as the TLR7/8 agonist,[16] and CpG oligodeoxynucleotides (CpG), and monophosphoryl lipid A (MPLA),[17−19] have been utilized to successfully improve the immunity in mice. However, substantially improving the immunogenicity of the antigen for subunit vaccines against COVID-19 still remains a challenging task.

As a potent immune activator for invariant natural killer T (iNKT) cells, α-galactosylceramide (αGalCer, also known as KRN7000) has been applied in many vaccine constructs.[20,21] iNKT cells are a unique subset of T lymphocytes with phenotypic markers of both T and natural killer (NK) cells.

Received: November 19, 2021

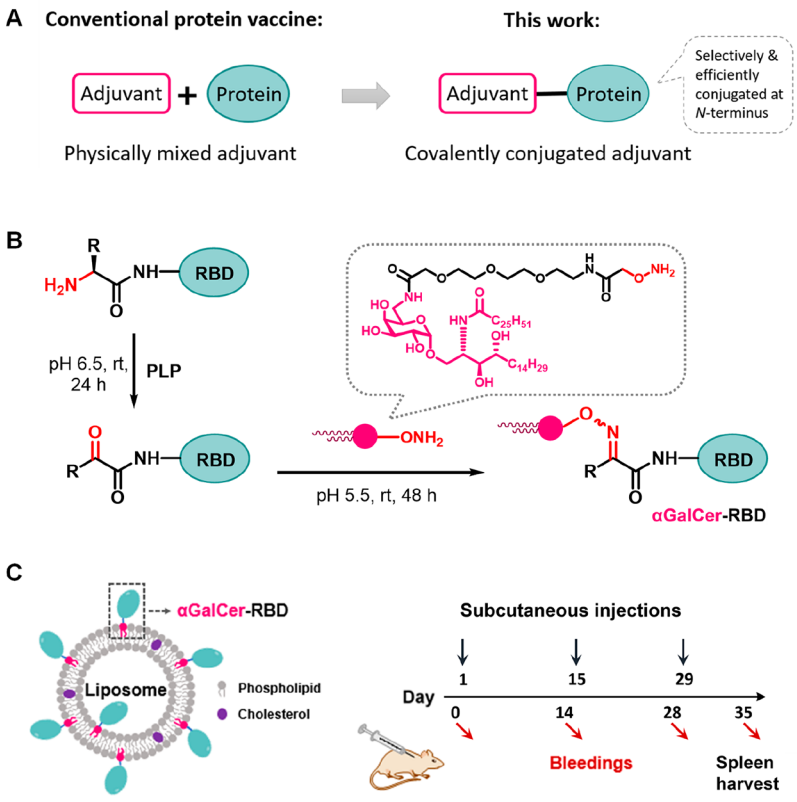

Figure 1. (A) Difference between the traditional protein vaccine design and that used in this work. (B) First, the RBD protein is incubated with pyridoxal 5′-phosphate (PLP), which transaminates the *N*-terminus of arginine to form a ketone. Second, the keto-protein reacts with alkoxyamine (αGalCer-linker) to form an oxime-linked protein−lipid conjugate. (C) Liposomal formulation of αGalCer-RBD was prepared before mice vaccination. 6−8 week old female BALB/c mice (n = 5 per group) were immunized subcutaneously on days 1, 15, and 29. Mice sera were collected on day 0 before initial immunization and on days 14, 28, and 35 after immunizations and splenocytes were isolated from vaccinated mice on day 35.

Straddling the innate and adaptive arms of the immune system, these cells modulate a wide range of immune effector properties. Once activated by αGalCer, iNKT cells release copious cytokines (IL-4 and IFN-γ) and license dendritic cells (DCs) to enhance their capacity to induce specific humoral and cellular responses.[22−24] In addition, iNKT cells may also directly help B cells to proliferate and undergo antibody class switching and affinity maturation.[25] Therefore, αGalCer and its derivatives are important adjuvants distinguished from those directly regulating conventional T cell-dependent immunogenic responses and are often used as admixed adjuvants in antitumor[26,27] and antiviral vaccines.[28] Besides, several studies have conjugated αGalCer with antigens such as small molecules,[29,30] carbohydrates,[31−33] and peptides[34−36] to develop potent self-adjuvanting vaccines. However, to date, αGalCer has not been reported to conjugate with protein antigens as a built-in stimulator.

Conventional protein-based subunit vaccines are often simply admixed with external adjuvants.[11−13] In this work, we developed a covalently conjugated adjuvant−protein vaccine that was easily prepared and highly effective (Figure 1A). For the first time, the iNKT cell agonist was conjugated to a protein antigen as a built-in stimulator. As the RBD is an immunodominant antigen of SARS-CoV-2 and accounts for 90% of the immune serum-neutralizing activity,[37] the RBD (S protein residues 319-541) was chosen as the protein antigen to develop the conjugate vaccine. Using a pyridoxal 5′-phosphate (PLP)-mediated transamination reaction, the *N*-terminus of the RBD protein was converted to the ketone and site-specifically conjugated with the adjuvant molecule via the oxime reaction (Figure 1B).[38,39] Herein, a single αGalCer molecule was covalently linked to the *N*-terminal amino acid (Arg) of the RBD, which was further prepared as liposomes for the use as a COVID-19 vaccine candidate. The co-delivery of the adjuvant and antigen was guaranteed by stable covalent conjugation; hence, the antigen-specific immune response could be boosted not only by the indirect CD4+ and CD8+ T cell stimulation but also by direct help toward B cells from iNKT cells.[40] Meanwhile, the conjugation approach would also affect the physical properties of the adjuvant. There are three major advantages of this conjugate vaccine: (1) simple and well-defined composition with a site-specific conjugation, (2) no interference of immunogenic epitopes on the antigen protein, and (3) potent efficiency with low adjuvant doses of liposomal formulation. In this study, we explored the effect of conjugation on humoral and cellular immune responses in mice and assessed its potential for developing an effective vaccine candidate against SARS-CoV-2 and variants of concern (VOCs).

RESULTS AND DISCUSSION

Preparation of Site-specifically Conjugated αGalCer-RBD. Our previous study has indicated that the immunogenicity of the antigen is significantly enhanced when the adjuvant molecule of the TLR7 agonist is covalently conjugated to the antigen-loaded protein.[41] In this study, the

https://doi.org/10.1021/acs.jmedchem.1c02000
J. Med. Chem. XXXX, XXX, XXX−XXX

Scheme 1. Reagents and Conditions are as follows: (A) (a) NaN_3 (3.0 equiv), H_2O, 80 °C, 8 h, 95%; (b) Ethyl Bromoacetate (1.2 equiv), NaH (1.2 equiv), THF, Reflux, 8 h, 73%; (c) PMe_3 (3.0 equiv), THF/H_2O (10:1, V/V), rt, 1 h; (d) Boc-Aminooxy Acetic Acid (2.0 equiv), EDC (3.0 equiv), DMAP (0.1 equiv), rt, 2 h, 61% Two Steps; and (e) 1 M NaOH, THF, rt, 3 h, 97%. (B) (a) TCl (1.5 equiv), Et_3N (2.0 equiv), CH_2Cl_2, 2 h; (b) NaN_3 (3.0 equiv), DMF, 80 °C, 5 h, 81% Two Steps; (c) $Pd(OH)_2/C$, $CH_2Cl_2/MeOH$, rt, 8 h; (d) 6 (2.0 equiv), HBTU (1.5 equiv), NMM (10 equiv), $CH_2Cl_2/MeOH$, rt, 2 h, 53% Two Steps; and (e) CH_2Cl_2/TFA, rt, 0.5 h, Quantitative Yield

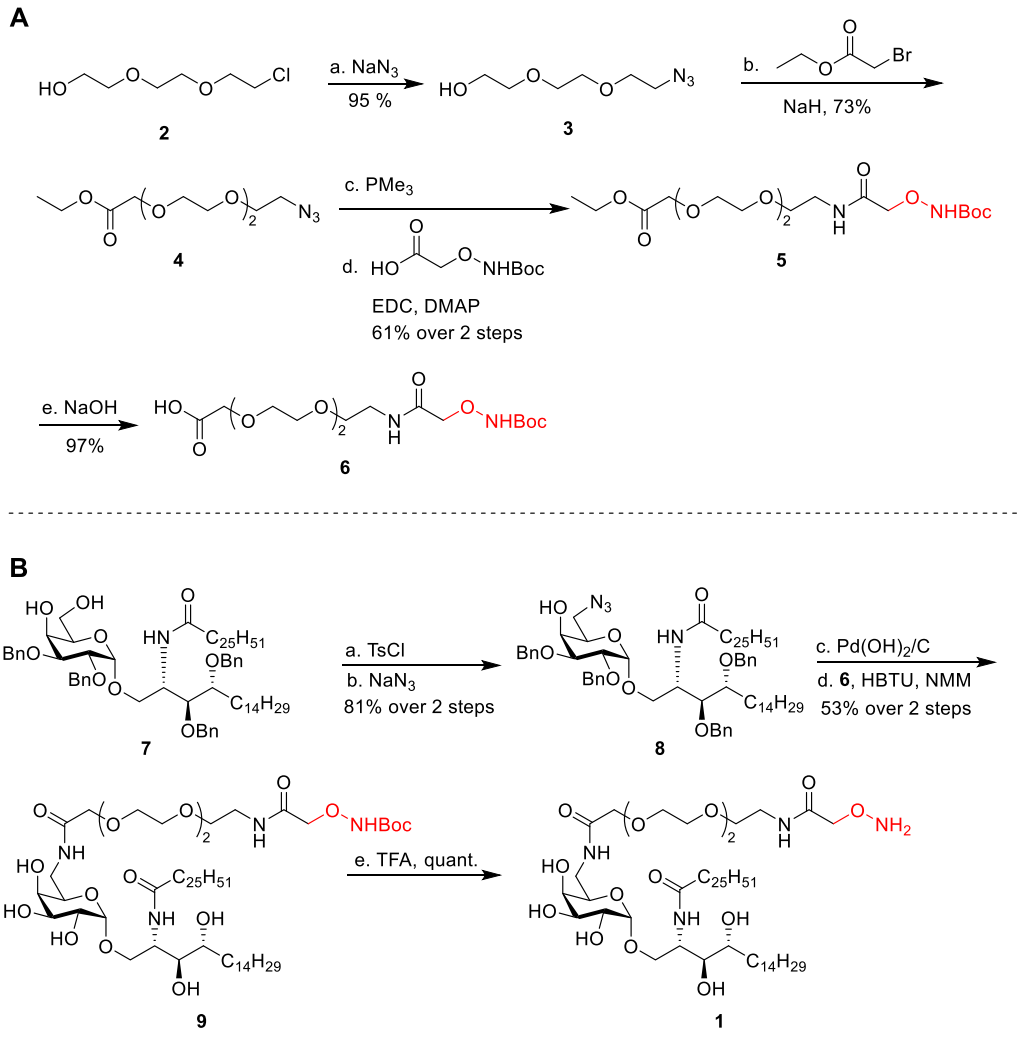

iNKT agonist αGalCer was covalently linked to the *N*-terminus of the protein for the first time. This site-specifically conjugated vaccine has minimal interference on immunogenic epitopes with a well-defined component. Although several studies have conjugated lipids on the protein using peptide ligation strategies to fuse lipopeptides on protein fragments[42,43] or chemical reactions to randomly attach adjuvants on the residues of protein, such as functionalization of lysine side chains,[44−48] these protein modification approaches can be difficult to control and need additional purification and the protein antigen epitopes are unavoidably interfered with, to a certain extent. Therefore, to prepare the αGalCer-RBD vaccine using a relatively simple transamination approach, the 6-position of αGalCer was modified with a linker with an alkoxyamine group (Scheme 1). First, to synthesize a alkoxyamine-modified linker, compound **3** was prepared by reacting 2-[2-(2-chloroethoxy)ethoxy] ethanol with sodium azide. The subsequent reaction of **3** with ethyl bromoacetate gave intermediate **4**. The azide was then reduced by the Staudinger reaction followed by a reaction with Boc-aminooxy acetic acid to afford **5**. Then, acid **6** was obtained by the hydrolysis of **5**. For the 6-position modification of αGalCer, compound **7** was first synthesized according to the method given in a previous report.[32] Then, the 6-OH group was effectively converted to an azide group by TsCl and NaN_3 to give azide-modified αGalCer **8**. After the removal of the Bn groups and the reduction of the azide group of **8** with $Pd(OH)_2/C$, acylation with linker **6** led to the αGalCer analogue **9**. The Boc group of compound **9** was removed to give αGalCer-ONH_2 **1**, with a high purity of 95% (Figure S11).

Next, the *N*-terminal residue of the RBD was site-specifically oxidized to a ketone group by pyridoxal 5′-phosphate (PLP)-mediated transamination. The imine intermediate formed by PLP and the *N*-terminus has an α proton with a much lower pK_a value, which allows the ketone to form uniquely at this site after the imine tautomerization and hydrolysis.[38,39] Then, the resulting ketone (the N-terminal residue is Arg in this case) was conjugated with one αGalCer-linker molecule by a stable oxime linkage (Figure 1B). The amino acid present in the *N*-terminus of the RBD is arginine, which is suitable for

https://doi.org/10.1021/acs.jmedchem.1c02000
J. Med. Chem. XXXX, XXX, XXX−XXX

conversion to ketone groups by PLP with good yield.[38,39] Analysis of the final αGalCer-RBD conjugate by MALDI-TOF mass spectrometry indicated that one αGalCer molecule covalently links with the RBD (Figure S3).

To evaluate the yield of the conjugation reaction, an RBD protein 319/321 fragment containing an Arg residue at its *N*-terminus was synthesized as a model tripeptide to conjugate with O-ethylhydroxylamine hydrochloride (Scheme S1).[49] The results of HPLC and ESI-MS analysis indicated a >95% overall yield of the conjugation reaction (Figure S1). Besides, the RBD protein was modified with a fluorescent biolabeling molecule, rhodamine B (RhB), on the *N*-terminus using PLP-mediated transamination (Scheme S2). RP-HPLC and SDS-PAGE analysis demonstrated a >85% overall yield of the RhB-RBD conjugation reaction (Figure S2). Therefore, the adjuvant−protein compound could be obtained in high yields through the transamination reaction.

Finally, the vaccine formulation was prepared as liposomes to further improve the aqueous solubility of the αGalCer-RBD conjugate or unconjugated RBD/αGalCer mixture (for characterization details, see Figure S4). As an ideal delivery system for vaccines, liposomes protect the antigen from degradation and can be efficiently taken up by DCs.[50,51] We also investigated liposomes encapsulating different protein subunits of the spike protein as effective COVID-19 vaccine candidates.[52] In the conjugate vaccine, the lipid tails of the αGalCer-RBD conjugate facilitate the anchoring of protein antigens on the liposome surface, mimicking lipoproteins anchored on the cell membrane, such as glycosylphosphatidylinositol (GPI) membrane anchors.[53] Meanwhile, the resulting liposomes biomimic the virus capsid structure that provides a multivalent effect of the antigen protein, thereby facilitating the recognition and uptake by the DCs with more effective activation.

Vaccination. The vaccines with the same RBD and/or αGalCer (10 μg RBD, 0.28 μg αGalCer for αGalCer-RBD or RBD/αGalCer) doses were immunologically evaluated in 6 to 8 week old female BALB/c mice. RBD alone (10 μg) and RBD (10 μg) plus alum adjuvant (100 μL) were used as negative and positive controls, respectively. αGalCer-RBD and RBD/αGalCer were further prepared in the form of liposomes with 1,2-distearoyl-*sn*-glycero-3-phosphocholine (DSPC) and cholesterol (50/40/1 molar ratio of DSPC/cholesterol/αGalCer-RBD or RBD/αGalCer). Five mice in each group were immunized subcutaneously (S.C.) on days 1, 15, and 29 (Figure 1C). Mice sera were collected on day 0 before initial immunization and days 14, 28, and 35 after immunizations, and splenocytes were isolated from vaccinated and untreated mice on day 35. In addition, another ten groups of mice were immunized S.C. or intraperitoneally (I.P.) with αGalCer-RBD, RBD/αGalCer, RBD/Al, RBD, and PBS for the evaluation of cytokine secretion and DC activation in vivo. For these groups, the doses of the antigen or adjuvant were set as 2 nmol (60 μg of RBD, 1.68 μg of αGalCer) for the S.C. route and 1 nmol (30 μg of RBD, 0.84 μg of αGalCer) for the I.P. route. Mice sera collected at 2 and 24 h after injection were evaluated for secretion of IL-4 and IFN-γ, respectively, and splenocytes were isolated 24 h after S.C. administration.

Conjugation Significantly Promoted Innate Immunity and RBD-Specific Antibody Responses. To investigate the impact of conjugated adjuvant on immune responses, we first evaluated cytokine secretion and DC activation in vivo. The results showed that a high level of IFN-γ was observed in the mice sera of αGalCer-RBD group 24 h after S.C. or I.P. injection (Figure S5A,B). In the intraperitoneally administered groups, the αGalCer-RBD-injected mice produced a ∼5-fold higher level of IFN-γ but slightly reduced IL-4 than that of αGalCer/RBD (Figure S5B,C), suggesting an enhanced Th1-biased immune response. Next, as DC maturation leads to the upregulation of co-stimulatory molecules (e.g., CD80, CD86, MHC I, and MHC II), the expression of CD86 was analyzed for the evaluation of iNKT cell-mediated DC activation in spleen 24 h after S.C. administration. The flow cytometry assay showed an increased expression of CD86 on CD11c + DCs (Figure 2), suggesting that αGalCer-RBD effectively activated

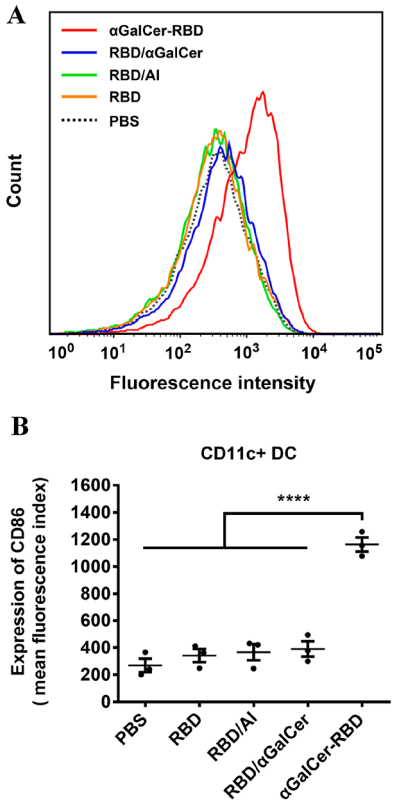

Figure 2. NKT cell-mediated activation of DCs in the spleen from mice 24 h after S.C. injection, as determined by evaluating the upregulation of CD86 as a marker of DC activation. (A) Histogram profiles for the CD86 expression on CD11c + DC cells. (B) MFI of CD86 on CD11c + DC cells. Data are shown as the mean ± SEM of three mice per group. Statistical significance was determined using one-way ANOVA with Dunn's multiple comparison test. $p < 0.0001$: ****, $p < 0.001$: ***, $p < 0.01$: **, and $p < 0.05$: *.

DCs mediated by iNKT cells. These results indicate that the conjugation approach altered the physical properties of αGalCer and thus improved the pharmacokinetic profiles, leading to greatly enhanced activation of innate immunity.

RBD antigen-specific antibody titers of each immunization were determined by ELISA. The IgM antibody titer of αGalCer-RBD-immunized mice was approximately equal to that of the control groups (Figure S6). However, the IgG antibody titer of αGalCer-RBD-immunized mice was 14.5-, 8.7-, and 5.9-fold higher than that of RBD-, RBD/Al-, and RBD/αGalCer-immunized mice on day 35, respectively (Figure 3A). The remarkable IgG antibody response initiated by αGalCer-RBD suggests that the conjugation of αGalCer

https://doi.org/10.1021/acs.jmedchem.1c02000
J. Med. Chem. XXXX, XXX, XXX−XXX

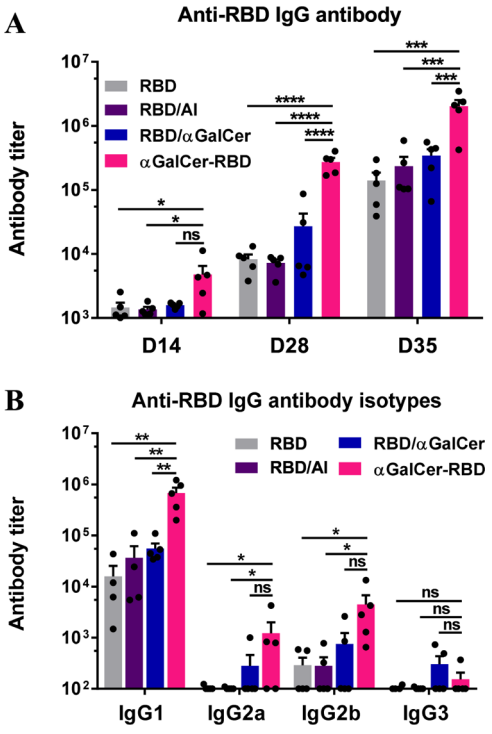

Figure 3. Adjuvant−protein conjugate promoted RBD-specific antibody responses. αGalCer-RBD and RBD/αGalCer were further prepared in the form of liposomes with DSPC and cholesterol at 50:40:1 (DSPC/cholesterol/αGalCer-RBD or RBD/αGalCer) molar ratios. (A) RBD-specific IgG antibody titers in serum samples from vaccinated mice on days 14, 28, and 35. (B) Anti-RBD IgG antibody isotypes in serum samples from vaccinated mice on day 35. Data are shown as the mean ± SEM of five mice per group and are representative of three separate experiments.

with the RBD significantly improves the immunogenicity of the protein antigen, which might be due to the co-delivery of the glycolipid adjuvant with the full protein to prime both B cells and T cells through cognate and noncognate help of iNKT cells.[54] High IgG titers in the αGalCer-RBD-administered mice after the first immunization indicate that adaptive immune responses were rapidly activated. Meanwhile, the αGalCer-RBD-immunized mice had elicited exceptionally higher IgG antibody titers than those of RBD- (33-fold), RBD/Al- (37-fold), and RBD/αGalCer (10-fold)-immunized mice on day 28 (Figure 3A). The rapid and strong humoral immune responses provoked by αGalCer-RBD after the second immunization suggests that a two-dose vaccination is enough to induce highly effective humoral immunity. αGalCer-RBD also showed high efficacy in inducing antibody class switching from IgM to RBD-specific IgG. These results indicate that covalently conjugating αGalCer and the antigen protein induces rapid and potent immune responses. In addition, the efficacy of αGalCer-RBD was still well-promoted by iNKT cells after restimulation, as the IgG titer increased 7.4-fold between the second and third immunizations, which is distinctive from the blunted antibody response of boosting immunizations with αGalCer-containing vaccines.[32,33]

The IgG subclass distribution of each group was primarily IgG1 (Figure 3B). Meanwhile, αGalCer-RBD-administered mice showed a more balanced enhancement of the Th1/Th2 response, with the IgG2a and IgG2b responses elicited being approximately 12- and 16-fold higher than those in the RBD/Al (Th2-biased)-immunized group, respectively. Hence, it is beneficial to use the αGalCer-RBD conjugate as a vaccine candidate against viral infections because the immune responses induced by such conjugate vaccines feature a broad IgG subclass distribution for effective protection.

αGalCer-RBD Conjugate Induced RBD-Specific, Cytokine-Producing T Cell Development. An effective vaccine against COVID-19 should induce not only humoral specific antibodies but also cellular immune responses to provide a full range of protective immunity.[55] To evaluate the RBD-specific cellular immune responses, splenocytes were collected from vaccinated mice one week after the last immunization, and the antigen-specific responses were measured by IFN-γ ELISPOT assay. The splenocytes were stimulated with 50 μg/mL overlapping peptide pool (spanning SARS-CoV-2-S RBD) for 18 h before forming IFN-γ spots. As shown in Figure 4A, αGalCer-RBD vaccination significantly increased the number of IFN-γ spots, with ∼4- and ∼26-fold increases in the number of IFN-γ spots compared to that after immunization with RBD/αGalCer and RBD/Al, respectively. Therefore, the conjugate vaccine enhanced cellular responses with increased numbers of antigen-specific cytokine-producing cells. To further characterize the contribution of these vaccine candidates to RBD-specific cellular immunity, cytokine-producing CD4+ (Figure 4F−H) and CD8+ (Figure 4C−E) T cells of splenocytes from immunized mice were evaluated by flow cytometry on day 35. As indicated in Figure 4C, 2.57, 1.32, and <1% CD8+ T cells derived from αGalCer-RBD-, RBD/αGalCer-, and RBD/Al-immunized mice, respectively, produced both IFN-γ and TNF-α cytokines following the stimulation of the overlapping peptide pool (spanning SARS-CoV-2-S RBD). A similar trend was observed for CD4+ T cells (Figure 4F) and IFN-γ+ or TNF-α+ cytokine-secreting cells (Figures 4D,E,G,H and S7). The specific cellular responses toward the RBD collectively confirmed that αGalCer-RBD provoked a potent cellular and humoral immune responses, implying that the αGalCer-RBD conjugate is a promising and effective candidate for the COVID-19 vaccine.

Pseudovirus and Live Virus Neutralizing Activity and Cross-Neutralization of Variants. Neutralizing antibody responses in mice were assessed against both wild-type (WT) pseudotyped and live SARS-CoV-2 virus. Furthermore, cross-neutralization assay of WT and all VOCs (B.1.1.7/alpha, B.1.351/beta, P.1/gamma, B.1.617.2/delta, and B.1.1.529/omicron) was evaluated using different pseudovirus assay approaches. WT pseudovirus neutralization ID_{50} ($pVNT_{50}$) of mice sera on day 35 is shown in Figure 5A. As expected, αGalCer-RBD vaccination generated the highest neutralizing antibody activity (mean $pVNT_{50}$ = 11,549), followed by that after vaccination with RBD/αGalCer (mean $pVNT_{50}$ = 3653), RBD/Al (mean $pVNT_{50}$ = 1553), and the RBD alone (mean $pVNT_{50}$ = 940). Similarly, the strongest neutralizing activity against live SARS-CoV-2 was detected in the αGalCer-RBD-vaccinated mice (Figure 5B), with a neutralization titer (NT_{50}) of 4529 on day 35 (Figure S8). Notably, it showed that compared with the WT group, anti-sera from αGalCer-RBD-immunized mice cross-neutralized the B.1.1.7 (1.1-fold decrease) and P.1 (1.4-fold decrease) variants efficiently but showed reduced responses against the B.1.351 (4.5-fold decrease), B.1.617.2 (2.4-fold decrease), and B.1.1.529 (13.9-fold decrease) variants (Figure 5C). These results are in line with previously reported results of mRNA and adenovirus vector-based vaccines.[56−59] The effective neutralization against

https://doi.org/10.1021/acs.jmedchem.1c02000
J. Med. Chem. XXXX, XXX, XXX−XXX

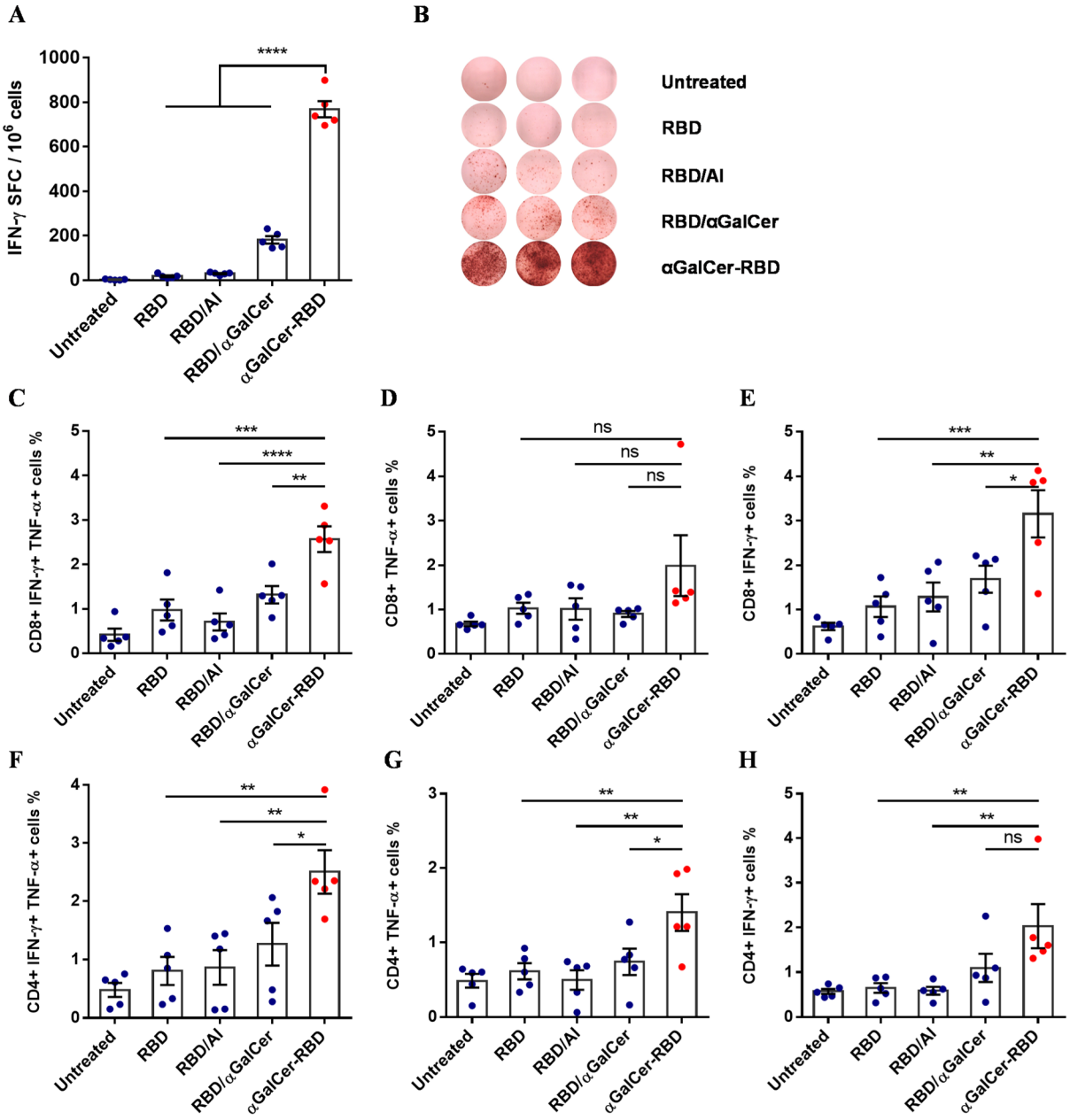

Figure 4. Adjuvant−protein conjugate induced potent RBD-specific cellular immune responses. Specific cytokine-producing T cell immune responses were assessed using splenocytes from immunized mice on day 35. (A) IFN-γ ELISpot assay. (B) Representative ELISpot wells. (C) Flow cytometry assay of IFN-γ and TNF-α double-positive cells in CD8+ T cells. (D) CD8+ TNF-α+ T cells, as a percentage of CD8+ T cells. (E) CD8+ IFN-γ+ T cells, as a percentage of CD8+ T cells. (F) Flow cytometry assay of IFN-γ and TNF-α double-positive cells in CD4+ T cells. (G) CD4+ TNF-α+ T cells, as a percentage of CD4+ T cells. (H) CD4+ IFN-γ+ T cells, as a percentage of CD4+ T cells. Data are shown as the mean ± SEM of five mice per group, each sample being characterized in triplicate. Statistical significance was determined using one-way ANOVA with Dunn's multiple comparison test. No significant difference: ns, $p < 0.0001$: ****, $p < 0.001$: ***, $p < 0.01$: **, and $p < 0.05$: *.

these variants indicates that αGalCer-RBD has the potential for the protection against SARS-CoV-2 and muted viruses as a candidate vaccine.

Anti-RBD Antibodies from αGalCer-RBD-Immunized Mice Effectively Blocked the Binding of RBD to ACE2. Sera collected on day 35 and pooled per group were also tested for their ability to inhibit the binding of the RBD protein to the ACE2-overexpressing HEK293 cells using flow cytometry (Figure 6). No mice serum was added to the positive control, and unstained cells were used as the negative control. The mean fluorescence intensity (MFI) of the cells incubated with the RBD-His protein without sera was defined as 100% binding.

Inhibition of binding was calculated as the percentage of reduced binding to the ACE2 receptor in the presence of diluted sera from mice immunized with different vaccine candidates. The results showed that mice sera (1/20 dilution) from αGalCer-RBD-, RBD/αGalCer-, and RBD/Al-immunized mice blocked the binding of the RBD to the ACE2 receptor at inhibition rates of 82, 41, and 32%, respectively. Thus, the anti-RBD antibodies induced in αGalCer-RBD-immunized mice had the strongest inhibition to suppress RBD-

https://doi.org/10.1021/acs.jmedchem.1c02000
J. Med. Chem. XXXX, XXX, XXX−XXX

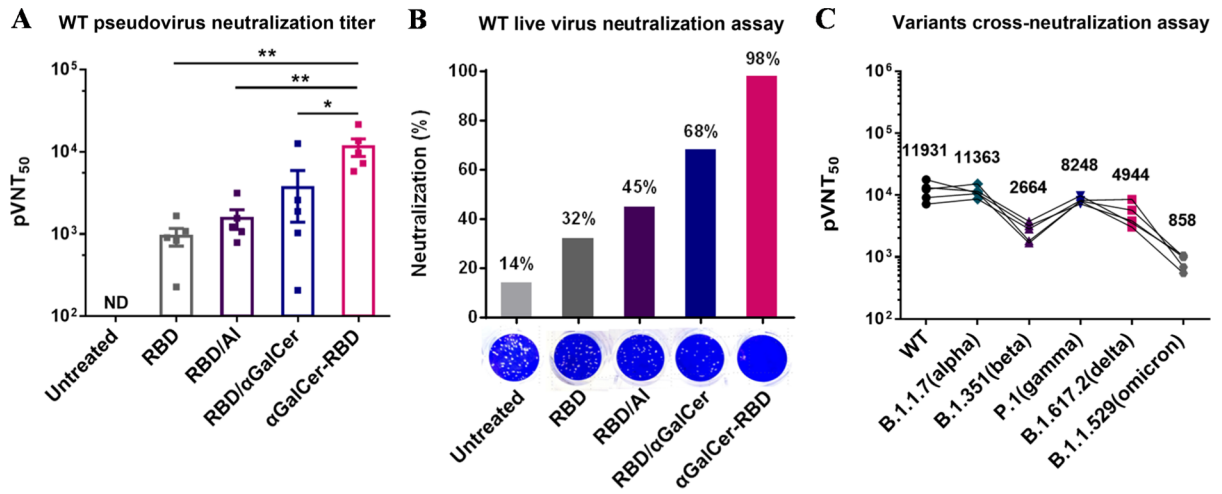

Figure 5. Enhanced neutralization of the SARS-CoV-2 pseudovirus and live virus by mice sera from αGalCer-RBD immunized mice. Mice sera collected on day 35 were serially diluted and analyzed for SARS-CoV-2 pseudotype particles and live SARS-CoV-2 neutralization. (A) Pseudovirus neutralization titers ($pVNT_{50}$). Data are shown as the mean ± SEM of $pVNT_{50}$ of five mice per group. ND: not detectable. Statistical significance was determined using one-way ANOVA with Dunn's multiple comparison test. $p < 0.01$: ** and $p < 0.05$: *. (B) Neutralization (%) of live SARS-CoV-2 in the presence of 1/400 diluted pooled sera using the plaque reduction neutralization test. Images are plaques formed in Vero E6 cells inoculated with live SARS-CoV-2. (C) Neutralization titers ($pVNT_{50}$) against B.1.1.7 (alpha), B.1.351 (beta), P.1 (gamma), B.1.617.2 (delta), and B.1.1.529 (omicron) pseudoviruses in the presence of serially diluted sera from the αGalCer-RBD immunized group. Data of a given sample for each mouse were linked to trace its neutralization titers against different pseudoviruses. Mean $pVNT_{50}$ values against different variants relative to the WT are shown and compared.

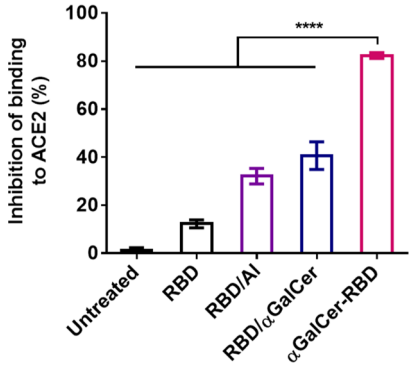

Figure 6. Strong inhibition of the RBD proteins binding to ACE2-HEK293 by mice sera from αGalCer-RBD immunized mice. Pooled serum samples (1/20 diluted) were collected on day 35 assayed for inhibition of the binding of the recombinant RBD-His protein to HEK293 cells overexpressing ACE2 by flow cytometry. In the positive control, no mice serum was added, and cells without any staining were used as a negative control. MFI values of the APC-A channel from cells incubated with the RBD-His protein without sera were defined as 100% binding. Inhibition of binding was calculated as the percentage of reduced binding to the ACE2 receptor in the presence of diluted sera from different immunization groups. Data are shown as the mean ± SEM of three independent experiments. Statistical significance was determined using one-way ANOVA with Dunn's multiple comparison test. $p < 0.0001$: ****, $p < 0.001$: ***, $p < 0.01$: **, and $p < 0.05$: *.

His binding to the ACE2 receptor and therefore exerted the most effective anti-RBD activity in vitro.

CONCLUSIONS

In summary, this study for the first time conjugates the iNKT cell agonist on the protein antigen, and the resulting αGalCer-RBD conjugate anchored on liposomes biomimicking the virus capsid structure remarkably enhances the protective immune response against SARS-CoV-2. Compared to the unconjugated RBD/αGalCer mixture, the αGalCer-RBD conjugate enhanced the immune efficacy of the adjuvant and produced significantly stronger humoral responses and cellular responses in mice. The rapid antibody response with two-dose immunization also makes the conjugate vaccine an applicable vaccine candidate for mass vaccination. Moreover, the antisera from αGalCer-RBD-immunized mice induced potent neutralizing responses with high pseudotyped neutralizing titers and live virus neutralization activity, indicating efficient protective immunity by this vaccine candidate. Meanwhile, the cross-neutralization of different SARS-CoV-2 VOCs (B.1.1.7/alpha, B.1.351/beta, P.1/gamma, B.1.617.2/delta, and B.1.1.529/omicron) by the αGalCer-RBD antisera suggests that this vaccine candidate could be of value in dealing with emerging variants. We expect that this novel promising vaccine design strategy using adjuvant−protein conjugates will have applications in various prophylactic or therapeutic vaccines against diseases and beyond.

EXPERIMENTAL SECTION

Chemical Synthesis. *General Information.* All reactions were carried out under a dry argon atmosphere using oven-dried glassware and magnetic stirring. The solvents were dried prior to use as follows: THF was heated at reflux over sodium benzophenone ketyl; CH_2Cl_2 was dried over CaH_2. Aluminum thin-layer chromatography (TLC) sheets (silica gel 60 F_{254}) of 0.2 mm thickness were used to monitor the reactions. The spots were visualized with short-wavelength UV light or by charring after spraying with a solution prepared from one of the following solutions: phosphomolybdic acid (5.0 g) in 95% EtOH (100 mL); *p*-anisaldehyde solution (2.5 mL of *p*-anisaldehyde, 2 mL of AcOH, and 3.5 mL of conc. H_2SO_4 in 100 mL of 95% EtOH); or ninhydrin solution (0.3 g of ninhydrin in 100 mL of n-butanol; add 3 mL of AcOH). Flash chromatography was carried out with silica gel 60 (230-400 ASTM mesh). αGalCer was prepared according to our reported procedure.[32] NMR spectra were obtained on a 400 or 600 MHz spectrometer. Chemical shifts were reported in parts per million (ppm). Electrospray ionization mass (ESI-MS) was performed on a TSQ Quantum Access MAX (Thermo Fisher

https://doi.org/10.1021/acs.jmedchem.1c02000
J. Med. Chem. XXXX, XXX, XXX−XXX

Scientific). High-resolution mass spectrometry (HRMS) was recorded on a Bruker micrOTOF II ESI-TOF using a positive electrospray ionization (ESI^+). Protein MALDI data were collected on a Bruker MALDI-TOF/TOF UltrafleXtreme spectrometer. The matrix used for MALDI-TOF was 3-(4-hydroxy-3,5-dimethoxyphenyl) prop-2-enoic acid. The HPLC data were obtained on an Agilent 1260 fitted with an evaporative light-scattering detector (ELSD). The purities of compounds **9** and **1** are >95%, as determined by HPLC-ELSD (see the Supporting Information).

*1-Azido-8-hydroxy-3,6-dioxaoctane (**3**).*[60] To a solution of NaN_3 (5.7 g, 88.9 mmol, 3.0 equiv) in water (40 mL) was added 2-[2-(2-chloroethoxy)ethoxy] ethanol (5.0 g, 29.6 mmol) under an argon atmosphere at rt. The reaction mixture was heated at 80 °C overnight. The crude mixture was extracted with CH_2Cl_2. The organic extracts were dried with anhydrous Na_2SO_4 and concentrated under reduced pressure to give a colorless oil (4.9 g, 95%), which was used without further purification. Spectra matched previously reported characterization data.[60] ^1H NMR (400 MHz, $CDCl_3$): δ 3.74 (q, J = 5.2 Hz, 2H), 3.69 (d, J = 4.2 Hz, 6H), 3.62 (t, J = 4.6 Hz, 2H), 3.41 (t, J = 5.0 Hz, 2H), 2.67 (t, J = 6.1 Hz, 1H). ^{13}C NMR (100 MHz, $CDCl_3$): δ 72.39, 70.48, 70.22, 69.88, 61.55, 50.48.

*Ethyl[2-(2-(2-azidoethoxy)ethoxy)ethoxy]acetate (**4**).* To a stirred suspension of compound **3** (2.0 g, 11.4 mmol) in dry THF (30 mL) were added ethyl bromoacetate (1.6 mL, 13.7 mmol, 1.2 equiv) and NaH (0.55 g, 13.7 mmol, 1.2 equiv) at 0 °C for 10 min under an argon atmosphere; then, the reaction mixture was refluxed for 8 h. After the completion of the reaction, monitored by TLC, the reaction mixture was added with H_2O (10 mL). The separated aqueous layer was extracted with CH_2Cl_2 (10 mL × 3). The organic extracts were dried with anhydrous Na_2SO_4 and concentrated under reduced pressure. The crude product was purified by silica gel column chromatography with ethyl acetate−petroleum ether (2:3) to give compound **4** as colorless oil (2.2 g, 73%). ^1H NMR (400 MHz, $CDCl_3$): δ 4.22 (q, J = 7.1 Hz, 2H), 4.15 (s, 2H), 3.77−3.71 (m, 4H), 3.70−3.66 (m, 6H), 3.40 (t, J = 5.1 Hz, 2H), 1.29 (t, J = 7.1 Hz, 3H). ^{13}C NMR (100 MHz, $CDCl_3$): δ 170.13, 70.56, 70.40, 70.34, 70.32, 69.75, 68.40, 68.38, 60.48, 60.46, 50.37, 13.91. MS (ESI): calcd for $C_{10}H_{19}N_3NaO_5$ $[M + Na]^+$, 284.12; found, 284.03.

*Ethyl 2,2-Dimethyl-4,8-dioxo-3,6,12,15,18-pentaoxa-5,9-diazaicosan-20-oate (**5**).* To a stirred solution of compound **4** (1.27 g, 4.86 mmol) in THF (10 mL) and H_2O (1 mL) was added PMe_3 (1 M in THF) (14.6 mL, 14.58 mmol, 3.0 equiv) under an argon atmosphere at rt for 2 h. After the completion of the reaction, monitored by TLC, the reaction mixture was evaporated under reduced pressure. The product was used in later reaction steps without further purification.

The crude product was dissolved in dry CH_2Cl_2 (20 mL). EDC·HCl (2.79 g, 14.58 mmol, 3.0 equiv), DMAP (59 mg, 0.486 mmol, 0.1 equiv), and Boc-aminooxy acetic acid (1.89 g, 9.72 mmol, 2.0 equiv) were added to the stirred mixture under an argon atmosphere at rt for 2 h. After the completion of the reaction, monitored by TLC, the reaction mixture was added with water (10 mL). The separated aqueous layer was extracted with CH_2Cl_2 (10 mL × 3). The organic extracts were dried with anhydrous Na_2SO_4 and concentrated under reduced pressure. The crude product was purified by silica gel column chromatography with CH_2Cl_2/MeOH (20:1) to give compound **5** as colorless oil (1.2 g, 61% yield over two steps): ^1H NMR (400 MHz, $CDCl_3$): δ 4.33 (s, 2H), 4.22 (qd, J = 7.2, 1.4 Hz, 2H), 4.16 (d, J = 1.4 Hz, 2H), 3.77−3.70 (m, 4H), 3.69−3.63 (m, 4H), 3.60 (t, J = 5.6 Hz, 2H), 3.50 (q, J = 5.6 Hz, 2H), 1.48 (d, J = 1.9 Hz, 9H), 1.29 (td, J = 7.2, 1.4 Hz, 3H). ^{13}C NMR (100 MHz, $CDCl_3$): δ 170.18, 168.98, 157.30, 81.85, 75.38, 70.44, 70.20, 70.11, 69.93, 69.17, 68.24, 60.52, 38.53, 27.82, 13.86. MS (ESI): calcd for $C_{17}H_{33}N_2O_9$ $[M + H]^+$, 409.21; found, 409.11.

*2,2-Dimethyl-4,8-dioxo-3,6,12,15,18-pentaoxa-5,9-diazaicosan-20-oic Acid (**6**).* To a stirred solution of compound **5** (80 mg, 0.19 mmol) in THF (4 mL) was added NaOH (1 M, 4 mL) at rt for 3 h. After the completion of the reaction, monitored by TLC, the reaction mixture was neutralized with 1 M HCl, and the whole sample was extracted with CH_2Cl_2 (3 mL) three times. The organic extracts were dried with anhydrous Na_2SO_4 and concentrated under reduced pressure to give compound **6** as colorless oil (70 mg, 97%): ^1H NMR (400 MHz, $CDCl_3$): δ 8.58 (s, 1H), 4.38 (s, 2H), 4.17 (s, 2H), 3.78−3.74 (m, 2H), 3.73−3.64 (m, 6H), 3.61 (t, J = 5.3 Hz, 2H), 3.52 (t, J = 5.4 Hz, 2H), 1.48 (s, 9H). ^{13}C NMR (100 MHz, $CDCl_3$): δ 172.61, 169.75, 157.65, 82.42, 75.39, 70.78, 70.28, 70.23, 69.96, 69.28, 68.31, 38.84, 27.99. MS (ESI): calcd for $C_{15}H_{27}N_2O_9$ $[M - H]^+$, 379.17; found, 379.06.

*N-((2S,3S,4R)-1-(((2S,3R,4S,5S,6R)-6-(Azidomethyl)-3,4-bis(benzyloxy)-5-hydroxytetrahydro-2-pyran-2-yl)oxy)-3,4-bis(benzyloxy)nonadecan-2-yl)hexacosanamide (**8**).* The preparation of compound **8** was carried out according to the method in the previous report.[32] To a solution of compound 7 (0.16 g, 0.13 mmol) in anhydrous CH_2Cl_2 (5 mL) were added Et_3N (36 μL, 0.26 mmol, 2.0 equiv) and TsCl (38 mg, 0.19 mmol, 1.5 equiv) at 0 °C for 10 min under an argon atmosphere; then, the mixture was warmed to rt and stirred for 2 h. After the completion of the reaction, monitored by TLC, the reaction mixture was washed with saturated aqueous NH_4Cl, and the whole sample was extracted with CH_2Cl_2 (10 mL × 3). The organic extracts were dried with anhydrous Na_2SO_4 and then concentrated under reduced pressure. The resulting residue was used in later reaction steps without further purification.

The crude product was dissolved in anhydrous DMF (10 mL) and NaN_3 (25 mg, 0.39 mmol, 3.0 equiv) was added to the stirred mixture at 80 °C for 5 h. After the completion of the reaction, monitored by TLC, the reaction mixture was diluted with CH_2Cl_2 (5 mL) and washed with H_2O (5 mL). The separated aqueous layer was washed with CH_2Cl_2 (5 mL × 3). The organic extracts were dried with anhydrous Na_2SO_4 and then concentrated under reduced pressure. The crude product was purified by silica gel column chromatography with ethyl acetate−petroleum ether (1:5) to give product **8** as a white foam (0.13 g, 81% yield over two steps): ^1H NMR (400 MHz, $CDCl_3$): δ 7.36−7.25 (m, 20H), 5.89 (d, J = 8.7 Hz, 1H), 4.83 (s, 1H), 4.73 (dt, J = 19.4, 11.4 Hz, 4H), 4.64−4.56 (m, 2H), 4.51 (dd, J = 11.7, 6.4 Hz, 2H), 4.34−4.26 (m, 1H), 3.91 (s, 1H), 3.85 (d, J = 5.1 Hz, 2H), 3.78 (d, J = 24.5 Hz, 4H), 3.61−3.49 (m, 2H), 3.30 (dd, J = 12.8, 4.8 Hz, 1H), 2.48 (s, 1H), 1.93 (q, J = 7.1 Hz, 2H), 1.72−1.61 (m, 4H), 1.53−1.37 (m, 4H), 1.24 (d, J = 6.5 Hz, 64H), 0.88 (t, J = 6.6 Hz, 6H). ^{13}C NMR (100 MHz, $CDCl_3$): δ 172.84, 138.53, 138.41, 138.04, 137.73, 128.54, 128.42, 128.35, 128.04, 127.93, 127.85, 127.77, 127.62, 127.57, 98.58, 79.64, 78.91, 75.62, 73.38, 73.09, 72.60, 71.71, 68.93, 68.52, 67.67, 51.16, 49.97, 36.72, 31.91, 29.81, 29.70, 29.62, 29.44, 29.36, 25.83, 25.71, 22.68, 14.13. MS (ESI): calcd for $C_{78}H_{123}N_4O_8$ $[M + H]^+$, 1243.93; found, 1243.57.

*tert-Butyl((1-((2R,3R,4S,5R,6S)-6-(((2S,3S,4R)-2-hexacosanamido-3,4-dihydroxynonadecyl)oxy)-3,4,5-trihydroxytetrahydro-2H-pyran-2-yl)-3,15-dioxo-5,8,11-trioxa-2,14-diazahexadecan-16-yl)oxy)carbamate (**9**).* A mixture of compound **8** (34 mg, 0.027 mmol) and $Pd(OH)_2/C$ (20% wt on carbon, 16 mg) in MeOH (3 mL) and CH_2Cl_2 (3 mL) was stirred for 8 h at rt under a H_2 atmosphere and then filtrated through a short pad of Celite with MeOH/CH_2Cl_2 (3:1). The filtrate was concentrated under reduced pressure to give a crude amine as a white solid. To a solution of the amine in anhydrous MeOH (2 mL) and CH_2Cl_2 (2 mL) were added **6** (20 mg, 0.054 mmol, 2.0 equiv), HBTU (15 mg, 0.041 mmol, 1.5 equiv), and NMM (30 μL, 0.27 mmol, 10 equiv) under an argon atmosphere at rt for 2 h. After the completion of the reaction, monitored by TLC, the solvent was evaporated under the reduced pressure. The resultant mixture was purified by silica gel flash column chromatography with CH_2Cl_2−MeOH (15:1) to give **9** as a white solid (17 mg, 53% yield over two steps, >95% pure by HPLC): ^1H NMR (400 MHz, $CDCl_3$/CD_3OD = 1:1, reference peak TMS at 0.00 ppm): δ 4.89 (d, J = 3.6 Hz, 1H), 4.30 (s, 2H), 4.18 (d, J = 5.0 Hz, 1H), 4.02 (d, J = 5.5 Hz, 2H), 3.84 (d, J = 3.0 Hz, 2H), 3.80 (dd, J = 13.2, 3.7 Hz, 1H), 3.75 (d, J = 3.1 Hz, 1H), 3.70 (d, J = 3.8 Hz, 8H), 3.65−3.60 (m, 5H), 3.58−3.53 (m, 3H), 3.50 (t, J = 5.5 Hz, 2H), 2.21 (t, J = 7.6 Hz, 2H), 1.64 (d, J = 13.2 Hz, 3H), 1.50 (s, 9H), 1.27 (s, 69H), 0.90 (d, J = 6.3 Hz, 6H). ^{13}C NMR (100 MHz, $CDCl_3$/CD_3OD = 1:1, reference peak CD_3OD at 49.00 ppm): δ 174.91, 172.24, 170.73, 158.80, 100.16, 82.68, 75.82, 74.83, 72.83, 72.39, 71.36, 70.83, 70.70, 70.62, 70.59,

https://doi.org/10.1021/acs.jmedchem.1c02000
J. Med. Chem. XXXX, XXX, XXX−XXX

70.43, 69.96, 69.78, 69.31, 69.21, 67.60, 63.80, 50.79, 39.82, 39.30, 36.89, 32.73, 32.39, 30.28, 30.25, 30.20, 30.18, 30.12, 30.09, 30.04, 29.93, 29.83, 29.81, 28.39, 26.41, 26.36, 23.12, 14.31. HRMS (ESI): calcd for $C_{65}H_{126}N_4NaO_{16}$ $[M + Na]^+$, 1241.9061; found, 1241.9010.

N-((2S,3S,4R)-1-(((2S,3R,4S,5R,6R)-6-(16-(Aminooxy)-3,15-dioxo-5,8,11-trioxa-2,14-diazahexadecyl)-3,4,5-trihydroxytetrahydro-2H-pyran-2-yl)oxy)-3,4-dihydroxynonadecan-2-yl)hexacosanamide (1). Compound **9** (4 mg, 3.28 μmol) was dissolved in CH_2Cl_2/TFA (10:1, 2 mL) at 0 °C, and the mixture was stirred for 0.5 h at rt under an argon atmosphere and then concentrated to dryness. The excess of TFA was removed by co-evaporation with CH_2Cl_2 under reduced pressure to give compound **1** as a white solid (3.6 mg, quantitative yield, >95% pure by HPLC), used in the next step without further purification. ^{1}H NMR (400 MHz, $CDCl_3/CD_3OD$ = 1:1, reference peak TMS at 0.00 ppm): δ 4.89 (d, *J* = 3.6 Hz, 1H), 4.16 (s, 2H), 4.05−3.96 (m, 2H), 3.84 (d, *J* = 6.2 Hz, 2H), 3.82−3.77 (m, 2H), 3.76 (s, 1H), 3.69 (t, *J* = 5.8 Hz, 10H), 3.61 (t, *J* = 5.0 Hz, 5H), 3.50 (t, *J* = 5.3 Hz, 2H), 2.22 (d, *J* = 5.8 Hz, 2H), 1.62 (s, 4H), 1.27 (s, 68H), 0.87 (s, 6H). ^{13}C NMR (100 MHz, $CDCl_3/CD_3OD$ = 1:1, reference peak CD_3OD at 49.00 ppm): δ 174.91, 172.24, 170.73, 100.16, 75.82, 74.83, 72.83, 72.39, 71.36, 70.83, 70.70, 70.62, 70.59, 70.43, 69.96, 69.78, 69.31, 69.21, 67.60, 63.80, 50.79, 39.82, 39.30, 36.89, 32.73, 32.39, 30.28, 30.25, 30.20, 30.18, 30.12, 30.09, 30.04, 29.93, 29.83, 29.81, 26.41, 26.36, 23.12, 14.31. HRMS (ESI): calcd for $C_{60}H_{118}N_4NaO_{14}$ $[M + Na]^+$, 1141.8537; found, 1141.8399.

αGalCer-RBD. The preparation of αGalCer-RBD was carried out according to the method in a previous report.[38,39] The RBD protein solution and PLP stock solution were combined in equal volumes to give a final concentration of 10 mM PLP and 10 μM RBD protein in PBS at pH 6.5. The reaction mixture was briefly agitated to ensure mixing and then incubated without further agitation at 37 °C for 24 h. Following the reaction, the PLP was removed using Amicon Ultrafiltration 0.5 mL units with a molecular weight cutoff (MWCO) of 10 kDa (Millipore). The sample was then concentrated to 100 μL after buffer exchange, and the process was repeated three times. The resulting 100 μL of keto-protein was treated with compound **1** (2 mM) in 1 mL of PBS/DMF (4:1, v/v, pH 5.5) and incubated at rt for 48 h. Buffer (containing 10% DMF) exchange steps were again repeated to stop the reaction and remove the excess adjuvant compound **1**. Since the lipid moiety of compound **1** is hydrophobic in aqueous buffer, the αGalCer-RBD conjugate and unreacted RBD protein were separated through centrifugation (1000*g*, 10 min, rt). The unreacted RBD in the supernatant was detected to calculate the conjugation reaction yield, which showed that the total yield was more than 85%. The high yield was in agreement with that of RhB-RBD (Figure S2). The purified αGalCer-RBD conjugate was then analyzed by MALDI-TOF mass spectrometry and used for the vaccine preparation.

Immunological Test. *Materials and Reagents.* Reagents used were RPMI-1640, DMEM (Gibco), and FBS (fetal bovine serum) (Gibco). The SARS-CoV-2-S-RBD was purchased from SinoBiological (40592-VNAH, 1.02 mg/mL in PBS, no His-tag). Bovine serum albumin (BSA) and the alum adjuvant (Alum) were purchased from Thermo Fisher Scientific. 1,2-Distearoyl-*sn*-glycero-3-phosphocholine (DSPC) was purchased from TCI. Cholesterol was purchased from Energy Chemical. Peroxidase-conjugated AffiniPure goat anti-mouse kappa, IgG1, IgG2a, IgG2b, and IgG3 antibodies were purchased from Southern Biotechnology, and peroxidase-conjugated AffiniPure goat anti-mouse kappa antibodies IgG and IgM were purchased from Jackson ImmunoResearch. The stable ACE2-HEK293 cell line was generated from HEK293 cells, which were transfected with an empty pCMV6-AC-GFP plasmid and a pCMV6-AC-GFP plasmid with a human ACE2 gene. The cells were selected by G418 (500 μg/mL). Monoclonal cell lines were derived by limited dilution. All animal experiments were performed at Laboratory Animal Centre of Huazhong Agriculture University (Wuhan, China). Animal experiments were conducted according to the animal ethics guidelines and following the recommendations concerning laboratory animal welfare.

Preparation and Characterization of Liposomes for Candidate Vaccines. Liposomal formulations of αGalCer-RBD and RBD/αGalCer were prepared by following previously reported protocols.[32,50] To prepare the liposomes for one dose, a mixture of DSPC (13.64 μg, 16.40 nmol) and cholesterol (5.34 μg, 13.12 nmol) (and αGalCer (0.28 μg, 0.33 nmol) for RBD/αGalCer liposomes) was dissolved in 2 mL of CH_2Cl_2/MeOH (1:1, v/v); the solvents were removed under reduced pressure through evaporation, which generated a thin lipid film on the flask wall. Then, αGalCer-RBD (62.16 μg, 1.97 nmol) (or RBD, 60 μg, 1.97 nmol) was added in the flask followed by overnight freeze drying. Next, 1.2 mL of PBS (pH 7.4) was added to hydrate the film, which was finally sonicated for 10 min and injected to mice (200 μL per mouse) immediately. The molar ratio of DSPC/cholesterol/antigen protein was 50:40:1. The average particle diameter and zeta potential were characterized using a Zetasizer Nano ZS instrument (Malvern) at rt.

In Vivo Cytokine Assay by ELISA. The cytokine levels in mice sera were assayed using ELISA kits (IFN-γ and IL-4, BD Pharmingen) according to the manufacturer's protocol. Briefly, 96-well plates (Costar type 3590, Corning Inc.) were coated with capture antibodies dissolved in the coating buffer per well and incubated at 4 °C overnight. The wells were then blocked with FBS for 1 h at rt. After blocking, 100 μL/well standard, sera, or control was added and incubated for 2 h at rt. After washing, the working detector (detection antibody and Sav-HRP reagent) was added to each well. The plates were incubated for 1 h at rt. Then, the plates were washed, and the tetramethyl benzidine (TMB) substrate solution was added for 30 min in the dark. The reactions were stopped with 2 N H_2SO_4 at rt. The absorbance was measured at 450 nm using a plate reader (BioTek, Synergy H1).

Analysis of Antibody Titers and Subtypes by ELISA. The RBD protein was dissolved in the prepared $NaHCO_3/Na_2CO_3$ buffer (50 mM, pH 9.5) with a final concentration of 1 μg/mL. Next, 96-well plates were coated with the RBD protein at 4 °C overnight. Then, the coated plates were washed three times with PBST (PBS + 0.1% Tween) and blocked with 2% BSA in PBS (100 μL/well) at 37 °C for 1 h. After washing three times, the plates were incubated with the serially diluted sera samples in PBS containing 0.1% BSA (100 μL/well) at 37 °C for 1 h. After other washing steps, the plates were incubated with one of the HRP-linked goat anti-mouse antibody IgG, IgM, IgG1, IgG2a, IgG2b, or IgG3, 1:5000 dilution in PBST (100 μL/well) at 37 °C for 1 h. After the final washing steps, TMB (500 μL, 0.2 mg/mL) in 9.5 mL of 0.05 M phosphate citrate buffer at pH 5.0 with 32 μL of 3% (w/v) urea hydrogen peroxide was added and allowed to react for 5 min in the dark. Next, the colorimetric reactions were terminated with 2.0 M H_2SO_4. Absorbance was recorded at 450 nm with a microplate reader (BioTek, Synergy H1).

Analysis of IFN-γ Secreting cells of Splenocytes by ELISPOT. IFN-γ secreting cells of splenocytes from each immunized group after the last boost were detected using ELISPOT kits (DAKEWE) according to the manufacturer's instructions. The 96-well plates were precoated with rat anti-mouse IFN-γ. A total of 200 μL of RPMI1640 without FBS was added to each well to activate the monoclonal antibodies. Splenocytes harvested from vaccinated mice were seeded into the wells (1×10^6 cells/well) in RPMI 1640 with 10% (v/v) FBS, 100 U/mL penicillin, and 100 μg/mL streptomycin containing 50 μg/mL peptide pool (GenScript, RP30020) (Spike, 1Met-643Phe, 158 peptides (15 mers with 11 aa overlap) spanning the SARS-CoV-2-S RBD) in duplicate. The cells were first cultured for 18 h at 37 °C and 5% CO_2 and then lysed with distilled H_2O for 10 min at 4 °C. After washing the plates six times, biotinylated anti-mouse IFN-γ antibodies (1:100) were added and incubated for 1 h at 37 °C. After other washing steps, the plates were incubated with streptavidin-HRP (1:100) for additional 1 h. After the final washing steps, AEC was added at 100 μL per well to develop spots in the dark for 30 min at rt; then, the reaction was quenched with distilled H_2O, and plates were air dried before counting.

Intracellular Cytokine Staining and Flow Cytometry. Cytokine-producing CD4+ and CD8+ T cells were evaluated in vitro with flow cytometry. Splenocytes of immunized mice after the last boost were

https://doi.org/10.1021/acs.jmedchem.1c02000
J. Med. Chem. XXXX, XXX, XXX−XXX

cultured in RPMI medium 1640 with 10% (v/v) FBS, 100 U/mL penicillin, and 100 μg/mL streptomycin containing 50 μg/mL peptide pool for 18 h. Brefeldin A (BD Biosciences) was administrated 12 h before staining to block intracellular cytokine secretion. Cells were then washed in stain buffer (1% BSA, 1% FBS and 0.1% (m/v) NaN_3 in PBS) and stained for 30 min at 4 °C with anti-CD3, anti-CD8, and anti-CD4 (all from BioLegend). Afterward, cells were fixed and permeabilized to facilitate intracellular staining with anti-IFN-γ and anti-IL-4 (BioLegend). For NKT-mediated DC activation assay, cells were stained with anti-CD11c and anti-CD86 (Biolegend). All labeled lymphocytes were gated on a FACSAriaIII flow cytometer (BD Biosciences).

Pseudovirus Neutralization Assay. Pseudovirus neutralization assay was performed using lentivirus-based SARS-CoV-2 pseudoviruses bearing WT (Genomeditech, GM-0220PV07) and B.1.1.7 (Genomeditech, GM-0220PV33), B.1.351 (Genomeditech, GM-0220PV32), P.1 (Genomeditech, GM-0220PV47), B.1.617.2 (Genomeditech, GM-0220PV45), and B.1.1.529/omicron (Genomeditech, GM-0220PV84) variant spike protein. Briefly, mouse sera were preheated at 56 °C for 30 min and serially diluted before incubating with 2×10^4 $TCID_{50}$ pseudoviruses for 1 h at rt in duplicate. The mixture was added to 2×10^4 HEK293T-ACE2 cells per well and incubated for 48 h of incubation in a 5% CO_2 environment at 37 °C. The luminescence was measured using a Bio-lite luciferase assay system (Genomeditech, G0483M001 and G0483M002) and detected for relative light units (RLUs) using a microplate reader (BioTek, Synergy H1). The titer of neutralization antibody ($pVNT_{50}$) was defined as the reciprocal serum dilution at which the RLUs were reduced by 50% compared to those in the virus control wells (virus + cells) after the subtraction of background RLUs in the control groups with cells only.

Live Virus Neutralization Assay. A plaque reduction neutralization test (PRNT) for live SARS-CoV-2 virus was developed as previously described.[61] Briefly, Vero E6 cells were seeded at 1.5×10^5 per well in a 24-well culture plate and grown overnight before use. Serial twofold dilutions of heat-inactivated (30 min at 56 °C) serum samples were prepared in DMEM medium. An equal volume of SARS-CoV-2 working stock containing 200 $TCID_{50}$ was added, and the serum−virus mixture was incubated at 37 °C for 1 h. The antibody−virus mixture was then added into the 24-well culture plate with the cell supernatant removed and incubated for 1 h at 37 °C. The serum−virus mixture was removed from Vero E6 cells followed by DMEM, and 0.9% carboxymethyl cellulose was overlaid. At 3 days after infection, cells were fixed and stained and then rinsed with water. Cells infected with SARS-CoV-2 were applied as the positive control. Neutralization (%) was calculated as the percentage of reduced plagues in the presence of 1/400 diluted sera from different vaccination groups. The neutralization titer (NT_{50}) was expressed as the reciprocal of the serum dilution that prevented the viral cytopathic effect in 50% of the wells. All the work with live SARS-CoV-2 virus was performed in a biosafety level 3 facility at the Wuhan Institute of Virology.

Analysis of Inhibition of RBD-His Binding to HEK293-ACE2 Cells. A FACS-based method was used to evaluate the inhibition rate of binding between RBD-His and HEK293-ACE2 cells. Briefly, freshly trypsinized ACE2-HEK293 cells in stain buffer (1% BSA, 1% FBS and 0.1% (m/v) NaN_3 in PBS) were added in 1.5 mL microcentrifuge tubes (1×10^6/tube) and then incubated with the recombinant spike RBD-His (0.5 μg/mL) protein and pooled sera (1/20 diluted) from immunized mice of each group for 1 h at 4 °C. Cells were then washed three times with PBS and stained with His-tag antibody iFluor 647 (GenScript) for 30 min. After another washing step, cells were analyzed on a FACSAriaIII flow cytometer (BD Biosciences).

Statistical Analyses. Comparison of multiple groups for statistical significance was carried out via one-way ANOVA with Tukey post hoc tests. Statistically significant responses are indicated by asterisks; data were analyzed using GraphPad Prism (GraphPad Software, San Diego, CA). Flow cytometry data were analyzed in Cytexpert 2.3 software.

■ ASSOCIATED CONTENT

Supporting Information

The Supporting Information is available free of charge at https://pubs.acs.org/doi/10.1021/acs.jmedchem.1c02000.

Transamination of model tripeptide; preparation of RhB-RBD; MALDI-TOF-MS analysis of αGalCer-RBD; characterization of vaccine liposomes; cytokine secretions in mice sera measured by ELISA; anti-RBD IgM antibody; flow cytometry assay; neutralization of pseudovirus and live SARS-CoV-2; compound NMR data; and purity assessment of the final compounds (PDF)

Molecular formula string data (CSV)

■ AUTHOR INFORMATION

Corresponding Authors

Rui Gong − *CAS Key Laboratory of Special Pathogens and Biosafety, Wuhan Institute of Virology, Center for Biosafety Mega-Science, Chinese Academy of Sciences, Wuhan 430071, China;* orcid.org/0000-0001-9222-5642; Email: gongr@wh.iov.cn

Guang-Fu Yang − *Key Laboratory of Pesticide & Chemical Biology of Ministry of Education, International Joint Research Center for Intelligent Biosensing Technology and Health, Hubei International Scientific and Technological Cooperation Base of Pesticide and Green Synthesis, College of Chemistry, Central China Normal University, Wuhan 430079, China;* orcid.org/0000-0003-4384-2593; Email: gfyang@mail.ccnu.edu.cn

Jun Guo − *Key Laboratory of Pesticide & Chemical Biology of Ministry of Education, International Joint Research Center for Intelligent Biosensing Technology and Health, Hubei International Scientific and Technological Cooperation Base of Pesticide and Green Synthesis, College of Chemistry, Central China Normal University, Wuhan 430079, China;* orcid.org/0000-0002-2097-5054; Email: jguo@mail.ccnu.edu.cn

Authors

Jian Wang − *Key Laboratory of Pesticide & Chemical Biology of Ministry of Education, International Joint Research Center for Intelligent Biosensing Technology and Health, Hubei International Scientific and Technological Cooperation Base of Pesticide and Green Synthesis, College of Chemistry, Central China Normal University, Wuhan 430079, China*

Yu Wen − *Key Laboratory of Pesticide & Chemical Biology of Ministry of Education, International Joint Research Center for Intelligent Biosensing Technology and Health, Hubei International Scientific and Technological Cooperation Base of Pesticide and Green Synthesis, College of Chemistry, Central China Normal University, Wuhan 430079, China*

Shi-Hao Zhou − *Key Laboratory of Pesticide & Chemical Biology of Ministry of Education, International Joint Research Center for Intelligent Biosensing Technology and Health, Hubei International Scientific and Technological Cooperation Base of Pesticide and Green Synthesis, College of Chemistry, Central China Normal University, Wuhan 430079, China*

Hai-Wei Zhang − *CAS Key Laboratory of Special Pathogens and Biosafety, Wuhan Institute of Virology, Center for Biosafety Mega-Science, Chinese Academy of Sciences, Wuhan 430071, China*

https://doi.org/10.1021/acs.jmedchem.1c02000
J. Med. Chem. XXXX, XXX, XXX−XXX

Xiao-Qian Peng − *Key Laboratory of Pesticide & Chemical Biology of Ministry of Education, International Joint Research Center for Intelligent Biosensing Technology and Health, Hubei International Scientific and Technological Cooperation Base of Pesticide and Green Synthesis, College of Chemistry, Central China Normal University, Wuhan 430079, China*

Ru-Yan Zhang − *Key Laboratory of Pesticide & Chemical Biology of Ministry of Education, International Joint Research Center for Intelligent Biosensing Technology and Health, Hubei International Scientific and Technological Cooperation Base of Pesticide and Green Synthesis, College of Chemistry, Central China Normal University, Wuhan 430079, China*

Xu-Guang Yin − *Key Laboratory of Pesticide & Chemical Biology of Ministry of Education, International Joint Research Center for Intelligent Biosensing Technology and Health, Hubei International Scientific and Technological Cooperation Base of Pesticide and Green Synthesis, College of Chemistry, Central China Normal University, Wuhan 430079, China*

Hong Qiu − *State Key Laboratory of Drug Research, Shanghai Institute of Materia Medica, Chinese Academy of Sciences, Shanghai 201203, China*

Complete contact information is available at: https://pubs.acs.org/10.1021/acs.jmedchem.1c02000

Author Contributions

[‖]J.W., Y.W., and S.-H.Z. contributed equally.

Notes

The authors declare no competing financial interest.

■ ACKNOWLEDGMENTS

We gratefully acknowledge the support of the National Natural Science Foundation of China (21772056 and 22177035), the National Key Research and Development Program of China (2017YFA0505200), the Wuhan Bureau of Science and Technology (2020020601012217 and 2020020101010001), the self-determined research funds of CCNU from the colleges' basic research and operation of MOE (CCNU20TS016), and the Program of Introducing Talents of Discipline to Universities of China (111 program, B17019).

■ ABBREVIATIONS

SARS-CoV-2, severe acute respiratory syndrome coronavirus 2; COVID-19, coronavirus disease 2019; RBD, receptor-binding domain; αGalCer, α-galactosylceramide; iNKT, invariant natural killer T; ACE2, angiotensin-converting enzyme 2; ADE, antibody-dependent enhancement; CDG, cyclic di-GMP; TLR, toll-like receptor; MPLA, monophosphoryl lipid A; NK, natural killer; DC, dendritic cell; IFN-γ, interferon-γ; IL-4, interleukin-4; PLP, pyridoxal 5′-phosphate; VOCs, variants of concern; GPI, glycosylphosphatidylinositol; WT, wild-type; ELSD, evaporative light scattering detector; DSPC, 1,2-distearoyl-*sn*-glycero-3-phosphocholine; EA, ethylacetate; ELISA, enzyme-linked immunosorbent assay; EDC, 1-ethyl-3-(3-(dimethylamino)propyl)-carbodiimide; FBS, fetal serum albumin; ICS, intracellular cytokine staining; PBS, phosphate-buffered saline; SEM, standard error of measurement

■ REFERENCES

(1) Jeyanathan, M.; Afkhami, S.; Smaill, F.; Miller, M. S.; Lichty, B. D.; Xing, Z. Immunological Considerations for COVID-19 Vaccine Strategies. *Nat. Rev. Immunol.* **2020**, *20*, 615−632.

(2) WHO. Draft Landscape of COVID-19 Candidate Vaccines. 2021, https://www.who.int/publications/m/item/draft-landscape-of-covid-19-candidate-vaccines.

(3) Ye, F.; Zhao, J.; Xu, P.; Liu, X.; Yu, J.; Wei, S.; Liu, J.; Xiaosheng Luo, X.; Li, C.; Ying, T.; Wang, J.; Yu, B.; Wang, P. Synthetic Homogeneous Glycoforms of the SARS-CoV-2 Spike Receptor-Binding Domain Reveals Different Binding Profiles of Monoclonal Antibodies. *Angew. Chem., Int. Ed.* **2021**, *60*, 2−9.

(4) Ortega-Rivera, O. A.; Shin, M. D.; Chen, A.; Beiss, V.; Moreno-Gonzalez, M. A.; Lopez-Ramirez, M. A.; Reynoso, M.; Wang, H.; Hurst, B. L.; Wang, J.; Pokorski, J. K.; Steinmetz, N. F. Trivalent Subunit Vaccine Candidates for COVID-19 and Their Delivery Devices. *J. Am. Chem. Soc.* **2021**, *143*, 14748.

(5) Yang, J.; Wang, W.; Chen, Z.; Lu, S.; Yang, F.; Bi, Z.; Bao, L.; Mo, F.; Li, X.; Huang, Y.; Hong, W.; Yang, Y.; Zhao, Y.; Ye, F.; Lin, S.; Deng, W.; Chen, H.; Lei, H.; Zhang, Z.; Luo, M.; Gao, H.; Zheng, Y.; Gong, Y.; Jiang, X.; Xu, Y.; Lv, Q.; Li, D.; Wang, M.; Li, F.; Wang, S.; Wang, G.; Yu, P.; Qu, Y.; Yang, L.; Deng, H.; Tong, A.; Li, J.; Wang, Z.; Yang, J.; Shen, G.; Zhao, Z.; Li, Y.; Luo, J.; Liu, H.; Yu, W.; Yang, M.; Xu, J.; Wang, J.; Li, H.; Wang, H.; Kuang, D.; Lin, P.; Hu, Z.; Guo, W.; Cheng, W.; He, Y.; Song, X.; Chen, C.; Xue, Z.; Yao, S.; Chen, L.; Ma, X.; Chen, S.; Gou, M.; Huang, W.; Wang, Y.; Fan, C.; Tian, Z.; Shi, M.; Wang, F.-S.; Dai, L.; Wu, M.; Li, G.; Wang, G.; Peng, Y.; Qian, Z.; Huang, C.; Lau, J. Y.-N.; Yang, Z.; Wei, Y.; Cen, X.; Peng, X.; Qin, C.; Zhang, K.; Lu, G.; Wei, X. A Vaccine Targeting the RBD of the S Protein of SARS-CoV-2 Induces Protective Immunity. *Nature* **2020**, *586*, 572−577.

(6) Dai, L.; Zheng, T.; Xu, K.; Han, Y.; Xu, L.; Huang, E.; An, Y.; Cheng, Y.; Li, S.; Liu, M.; Yang, M.; Li, Y.; Cheng, H.; Yuan, Y.; Zhang, W.; Ke, C.; Wong, G.; Qi, J.; Qin, C.; Yan, J.; Gao, G. F. A Universal Design of Betacoronavirus Vaccines against COVID-19, MERS, and SARS. *Cell* **2020**, *182*, 722−733.

(7) Walls, A. C.; Fiala, B.; Schäfer, A.; Wrenn, S.; Pham, M. N.; Murphy, M.; Tse, L. V.; Shehata, L.; O'Connor, M. A.; Chen, C.; Navarro, M. J.; Miranda, M. C.; Pettie, D.; Ravichandran, R.; Kraft, J. C.; Ogohara, C.; Palser, A.; Chalk, S.; Lee, E.-C.; Guerriero, K.; Kepl, E.; Chow, C. M.; Sydeman, C.; Hodge, E. A.; Brown, B.; Fuller, J. T.; Dinnon, K. H.; Gralinski, L. E.; Leist, S. R.; Gully, K. L.; Lewis, T. B.; Guttman, M.; Chu, H. Y.; Lee, K. K.; Fuller, D. H.; Baric, R. S.; Kellam, P.; Carter, L.; Pepper, M.; Sheahan, T. P.; Veesler, D.; King, N. P. Elicitation of Potent Neutralizing Antibody Responses by Designed Protein Nanoparticle Vaccines for SARS-CoV-2. *Cell* **2020**, *183*, 1367−1382.

(8) Liu, Z.; Xu, W.; Xia, S.; Gu, C.; Wang, X.; Wang, Q.; Zhou, J.; Wu, Y.; Cai, X.; Qu, D.; Ying, T.; Xie, Y.; Lu, L.; Yuan, Z.; Jiang, S. RBD-Fc-based COVID-19 Vaccine Candidate Induces Highly Potent SARS-CoV-2 Neutralizing Antibody Response. *Signal Transduction Targeted Ther.* **2020**, *5*, 282.

(9) Lee, W. S.; Wheatley, A. K.; Kent, S. J.; DeKosky, B. J. Antibody-Dependent Enhancement and SARS-CoV-2 Vaccines and Therapies. *Nat. Microbiol.* **2020**, *5*, 1185−1191.

(10) Spaninger, E.; Bren, U. Carcinogenesis of beta-Propiolactone: A Computational Study. *Chem. Res. Toxicol.* **2020**, *33*, 769−781.

(11) Li, Q.; Guo, Z. Recent Advances in Toll Like Receptor-Targeting Glycoconjugate Vaccines. *Molecules* **2018**, *23*, 1583.

(12) Lu, B. L.; Williams, G. M.; Brimble, M. A. TLR2 Agonists and Their Structure-Activity Relationships. *Org. Biomol. Chem.* **2020**, *18*, 5073−5094.

(13) Li, W.-H.; Li, Y.-M. Chemical Strategies to Boost Cancer Vaccines. *Chem. Rev.* **2020**, *120*, 11420−11478.

(14) Peng, S.; Cao, F.; Xia, Y.; Gao, X. D.; Dai, L.; Yan, J.; Ma, G. Particulate Alum via Pickering Emulsion for an Enhanced COVID-19 Vaccine Adjuvant. *Adv. Mater.* **2020**, *32*, No. e2004210.

(15) Wu, J.-J.; Zhao, L.; Han, B.-B.; Hu, H.-G.; Zhang, B.-D.; Li, W.-H.; Chen, Y.-X.; Li, Y.-M. A Novel STING Agonist for Cancer Immunotherapy and a SARS-CoV-2 Vaccine Adjuvant. *Chem. Commun.* **2021**, *57*, 504−507.

(16) Jangra, S.; De Vrieze, J.; Choi, A.; Rathnasinghe, R.; Laghlali, G.; Uvyn, A.; Van Herck, S.; Nuhn, L.; Deswarte, K.; Zhong, Z.;

Sanders, N.; Lienenklaus, S.; David, S.; Strohmeier, S.; Amanat, F.; Krammer, F.; Hammad, H.; Lambrecht, B. N.; Coughlan, L.; Garcia-Sastre, A.; de Geest, B.; Schotsaert, M. Sterilizing Immunity Against SARS-CoV-2 Infection in Mice by a Single-Shot and Lipid Amphiphile Imidazoquinoline TLR7/8 Agonist-Adjuvanted Recombinant Spike Protein Vaccine. *Angew. Chem., Int. Ed.* **2021**, *60*, 9467.

(17) Steinbuck, M. P.; Seenappa, L. M.; Jakubowski, A.; McNeil, L. K.; Haqq, M. C.; DeMuth, P. C. A Lymph Node-Targeted Amphiphile Vaccine Induces Potent Cellular and Humoral Immunity to SARS-CoV-2. *Sci. Adv.* **2021**, *7*, No. eabe5819.

(18) Liu, L.; Liu, Z.; Chen, H.; Liu, H.; Gao, Q.; Cong, F.; Gao, G.; Chen, Y. Subunit Nanovaccine with Potent Cellular and Mucosal Immunity for COVID-19. *ACS Appl. Bio Mater.* **2020**, *3*, 5633−5638.

(19) Park, K. S.; Bazzill, J. D.; Son, S.; Nam, J.; Shin, S. W.; Ochyl, L. J.; Stuckey, J. A.; Meagher, J. L.; Chang, L.; Song, J.; Montefiori, D. C.; LaBranche, C. C.; Smith, J. L.; Xu, J.; Moon, J. J. Lipid-Based Vaccine Nanoparticles for Induction of Humoral Immune Responses Against HIV-1 and SARS-CoV-2. *J. Control. Release* **2021**, *330*, 529−539.

(20) Cerundolo, V.; Silk, J. D.; Masri, S. H.; Salio, M. Harnessing Invariant NKT Cells in Vaccination Strategies. *Nat. Rev. Immunol.* **2009**, *9*, 28−38.

(21) Kharkwal, S. S.; Arora, P.; Porcelli, S. A. Glycolipid Activators of Invariant NKT Cells as Vaccine Adjuvants. *Immunogenetics* **2016**, *68*, 597−610.

(22) Liu, Z.; Guo, J. NKT-cell Glycolipid Agonist as Adjuvant in Synthetic Vaccine. *Carbohydr. Res.* **2017**, *452*, 78−90.

(23) Painter, G. F.; Burn, O. K.; Hermans, I. F. Using Agonists for iNKT Cells in Cancer Therapy. *Mol. Immunol.* **2021**, *130*, 1−6.

(24) Speir, M.; Hermans, I. F.; Weinkove, R. Engaging Natural Killer T Cells as 'Universal Helpers' for Vaccination. *Drugs* **2017**, *77*, 1−15.

(25) Barral, P.; Eckl-Dorna, J.; Harwood, N. E.; De Santo, C.; Salio, M.; Illarionov, P.; Besra, G. S.; Cerundolo, V.; Batista, F. D. B Cell Receptor-Mediated Uptake of CD1d-Restricted Antigen Augments Antibody Responses by Recruiting Invariant NKT Cell Help in vivo. *Proc. Natl. Acad. Sci. U.S.A.* **2008**, *105*, 8345−8350.

(26) Huang, Y.-L.; Hung, J.-T.; Cheung, S. K. C.; Lee, H.-Y.; Chu, K.-C.; Li, S.-T.; Lin, Y.-C.; Ren, C.-T.; Cheng, T.-J. R.; Hsu, T.-L.; Yu, A. L.; Wu, C.-Y.; Wong, C.-H. Carbohydrate-Based Vaccines with a Glycolipid Adjuvant for Breast Cancer. *Proc. Natl. Acad. Sci. U.S.A.* **2013**, *110*, 2517−2522.

(27) Deng, S.; Bai, L.; Reboulet, R.; Matthew, R.; Engler, D. A.; Teyton, L.; Bendelac, A.; Savage, P. B. A Peptide-Free, Liposome-Based Oligosaccharide Vaccine, Adjuvanted with a Natural Killer T Cell Antigen, Generates Robust Antibody Responses in vivo. *Chem. Sci.* **2014**, *5*, 1437−1441.

(28) Artiaga, B. L.; Yang, G.; Hackmann, T. J.; Liu, Q.; Richt, J. A.; Salek-Ardakani, S.; Castleman, W. L.; Lednicky, J. A.; Driver, J. P. alpha-Galactosylceramide Protects Swine Against Influenza Infection when Administered as a Vaccine Adjuvant. *Sci. Rep.* **2016**, *6*, 23593.

(29) Leadbetter, E. A.; Brigl, M.; Illarionov, P.; Cohen, N.; Luteran, M. C.; Pillai, S.; Besra, G. S.; Brenner, M. B. NKT Cells Provide Lipid Antigen-Specific Cognate Help for B Cells. *Proc. Natl. Acad. Sci. U.S.A.* **2008**, *105*, 8339−8344.

(30) Chen, X.-Z.; Zhang, R.-Y.; Wang, X.-F.; Yin, X.-G.; Wang, J.; Wang, Y.-C.; Liu, X.; Du, J.-J.; Liu, Z.; Guo, J. Peptide-Free Synthetic Nicotine Vaccine Candidates with alpha-Galactosylceramide as Adjuvant. *Mol. Pharm.* **2019**, *16*, 1467−1476.

(31) Cavallari, M.; Stallforth, P.; Kalinichenko, A.; Rathwell, D. C. K.; Gronewold, T. M. A.; Adibekian, A.; Mori, L.; Landmann, R.; Seeberger, P. H.; De Libero, G. A Semisynthetic Carbohydrate-Lipid Vaccine that Protects Against S. Pneumoniae in Mice. *Nat. Chem. Biol.* **2014**, *10*, 950−956.

(32) Yin, X.-G.; Chen, X.-Z.; Sun, W.-M.; Geng, X.-S.; Zhang, X.-K.; Wang, J.; Ji, P.-P.; Zhou, Z.-Y.; Baek, D. J.; Yang, G.-F.; Liu, Z.; Guo, J. IgG Antibody Response Elicited by a Fully Synthetic Two-Component Carbohydrate-Based Cancer Vaccine Candidate with α-Galactosylceramide as Built-in Adjuvant. *Org. Lett.* **2017**, *19*, 456−459.

(33) Yin, X.-G.; Lu, J.; Wang, J.; Zhang, R.-Y.; Wang, X.-F.; Liao, C.-M.; Liu, X.-P.; Liu, Z.; Guo, J. Synthesis and Evaluation of Liposomal anti-GM3 Cancer Vaccine Candidates Covalently and Noncovalently Adjuvanted by αGalCer. *J. Med. Chem.* **2021**, *64*, 1951−1965.

(34) Anderson, R. J.; Tang, C.-w.; Daniels, N. J.; Compton, B. J.; Hayman, C. M.; Johnston, K. A.; Knight, D. A.; Gasser, O.; Poyntz, H. C.; Ferguson, P. M.; Larsen, D. S.; Ronchese, F.; Painter, G. F.; Hermans, I. F. A Self-Adjuvanting Vaccine Induces Cytotoxic T Lymphocytes that Suppress Allergy. *Nat. Chem. Biol.* **2014**, *10*, 943−949.

(35) Compton, B. J.; Tang, C.-w.; Johnston, K. A.; Osmond, T. L.; Hayman, C. M.; Larsen, D. S.; Hermans, I. F.; Painter, G. F. Synthesis and Activity of 6″-Deoxy-6″-thio-α-GalCer and Peptide Conjugates. *Org. Lett.* **2015**, *17*, 5954−5957.

(36) Chen, P. G.; Hu, H. G.; Sun, Z. Y.; Li, Q. Q.; Zhang, B. D.; Wu, J. J.; Li, W. H.; Zhao, Y. F.; Chen, Y. X.; Li, Y. M. Fully Synthetic Invariant NKT Cell-Dependent Self-Adjuvanting Antitumor Vaccines Eliciting Potent Immune Response in Mice. *Mol. Pharm.* **2020**, *17*, 417−425.

(37) Piccoli, L.; Park, Y.-J.; Tortorici, M. A.; Czudnochowski, N.; Walls, A. C.; Beltramello, M.; Silacci-Fregni, C.; Pinto, D.; Rosen, L. E.; Bowen, J. E.; Acton, O. J.; Jaconi, S.; Guarino, B.; Minola, A.; Zatta, F.; Sprugasci, N.; Bassi, J.; Peter, A.; De Marco, A.; Nix, J. C.; Mele, F.; Jovic, S.; Rodriguez, B. F.; Gupta, S. V.; Jin, F.; Piumatti, G.; Lo Presti, G.; Pellanda, A. F.; Biggiogero, M.; Tarkowski, M.; Pizzuto, M. S.; Cameroni, E.; Havenar-Daughton, C.; Smithey, M.; Hong, D.; Lepori, V.; Albanese, E.; Ceschi, A.; Bernasconi, E.; Elzi, L.; Ferrari, P.; Garzoni, C.; Riva, A.; Snell, G.; Sallusto, F.; Fink, K.; Virgin, H. W.; Lanzavecchia, A.; Corti, D.; Veesler, D. Mapping Neutralizing and Immunodominant Sites on the SARS-CoV-2 Spike Receptor-Binding Domain by Structure-Guided High-Resolution Serology. *Cell* **2020**, *183*, 1024−1042.

(38) Gilmore, J. M.; Scheck, R. A.; Esser-Kahn, A. P.; Joshi, N. S.; Francis, M. B. N-Terminal Protein Modification through a Biomimetic Transamination Reaction. *Angew. Chem., Int. Ed.* **2006**, *45*, 5307−5311.

(39) Witus, L. S.; Moore, T.; Thuronyi, B. W.; Esser-Kahn, A. P.; Scheck, R. A.; Iavarone, A. T.; Francis, M. B. Identification of Highly Reactive Sequences for PLP-Mediated Bioconjugation Using a Combinatorial Peptide Library. *J. Am. Chem. Soc.* **2010**, *132*, 16812−16817.

(40) Fujii, S.-i.; Yamasaki, S.; Sato, Y.; Shimizu, K. Vaccine Designs Utilizing Invariant NKT-Licensed Antigen-Presenting Cells Provide NKT or T Cell Help for B Cell Responses. *Front. Immunol.* **2018**, *9*, 1267.

(41) Du, J.-J.; Wang, C.-W.; Xu, W.-B.; Zhang, L.; Tang, Y.-K.; Zhou, S.-H.; Gao, X.-F.; Yang, G.-F.; Guo, J. Multifunctional Protein Conjugates with Built-in Adjuvant (Adjuvant-Protein-Antigen) as Cancer Vaccines Boost Potent Immune Responses. *iScience* **2020**, *23*, 100935.

(42) Xu, Z.; Rivera-Hernandez, T.; Moyle, P. M. Development of an Enzyme-Mediated, Site-Specific Method to Conjugate Toll-Like Receptor 2 Agonists onto Protein Antigens: Toward a Broadly Protective, Four Component, Group A Streptococcal Self-Adjuvanting Lipoprotein-Fusion Combination Vaccine. *ACS Infect. Dis.* **2020**, *6*, 1770−1782.

(43) Hanna, C. C.; Ashhurst, A. S.; Quan, D.; Maxwell, J. W. C.; Britton, W. J.; Payne, R. J. Synthetic Protein Conjugate Vaccines Provide Protection Against Mycobacterium Tuberculosis in Mice. *Proc. Natl. Acad. Sci. U.S.A.* **2021**, *118*, No. e2013730118.

(44) Schülke, S.; Vogel, L.; Junker, A. C.; Hanschmann, K. M.; Flaczyk, A.; Vieths, S.; Scheurer, S. A Fusion Protein Consisting of the Vaccine Adjuvant Monophosphoryl Lipid A and the Allergen Ovalbumin Boosts Allergen-Specific Th1, Th2, and Th17 Responses in Vitro. *J. Immunol. Res.* **2016**, *2016*, 4156456.

(45) Kramer, K.; Young, S. L.; Walker, G. F. Comparative Study of 5'- and 3'-Linked CpG-Antigen Conjugates for the Induction of Cellular Immune Responses. *ACS Omega* **2017**, *2*, 227−235.

https://doi.org/10.1021/acs.jmedchem.1c02000
J. Med. Chem. XXXX, XXX, XXX−XXX

(46) Clauson, R. M.; Berg, B.; Chertok, B. The Content of CpG-DNA in Antigen-CpG Conjugate Vaccines Determines Their Cross-Presentation Activity. *Bioconjugate Chem.* **2019**, *30*, 561−567.
(47) Wilson, D. S.; Hirosue, S.; Raczy, M. M.; Bonilla-Ramirez, L.; Jeanbart, L.; Wang, R.; Kwissa, M.; Franetich, J.-F.; Broggi, M. A. S.; Diaceri, G.; Quaglia-Thermes, X.; Mazier, D.; Swartz, M. A.; Hubbell, J. A. Antigens Reversibly Conjugated to a Polymeric Glyco-Adjuvant Induce Protective Humoral and Cellular Immunity. *Nat. Mater.* **2019**, *18*, 175−185.
(48) Massena, C. J.; Lathrop, S. K.; Davison, C. J.; Schoener, R.; Bazin, H. G.; Evans, J. T.; Burkhart, D. J. A Tractable Covalent Linker Strategy for the Production of Immunogenic Antigen-TLR7/8L Bioconjugates. *Chem. Commun.* **2021**, *57*, 4698−4701.
(49) Wang, S.; Zhou, Q.; Chen, X.; Luo, R.-H.; Li, Y.; Liu, X.; Yang, L.-M.; Zheng, Y.-T.; Wang, P. Modification of N-terminal α-Amine of Proteins via Biomimetic Ortho-Quinone-Mediated Oxidation. *Nat. Commun.* **2021**, *12*, 2257.
(50) Du, J.-J.; Zou, S.-Y.; Chen, X.-Z.; Xu, W.-B.; Wang, C.-W.; Zhang, L.; Tang, Y.-K.; Zhou, S.-H.; Wang, J.; Yin, X.-G.; Gao, X.-F.; Liu, Z.; Guo, J. Liposomal Antitumor Vaccines Targeting Mucin 1 Elicit a Lipid-Dependent Immunodominant Response. *Chem.-Asian J.* **2019**, *14*, 2116−2121.
(51) Antimisiaris, S. G.; Marazioti, A.; Kannavou, M.; Natsaridis, E.; Gkartziou, F.; Kogkos, G.; Mourtas, S. Overcoming barriers by local drug delivery with liposomes. *Adv. Drug Delivery Rev.* **2021**, *174*, 53−86.
(52) Wang, J.; Yin, X. G.; Wen, Y.; Lu, J.; Zhang, R. Y.; Zhou, S. H.; Liao, C. M.; Wei, H. W.; Guo, J. *MPLA-Adjuvanted Liposomes Encapsulating S-trimer or RBD or S1, But Not S-ECD, Elicit Robust Neutralization against SARS-CoV-2 and Variants of Concern*. Accepted.
(53) Yu, S.; Guo, Z.; Johnson, C.; Gu, G.; Wu, Q. Recent Progress in Synthetic and Biological Studies of GPI Anchors and GPI-Anchored Proteins. *Curr. Opin. Chem. Biol.* **2013**, *17*, 1006−1013.
(54) King, I. L.; Fortier, A.; Tighe, M.; Dibble, J.; Watts, G. F. M.; Veerapen, N.; Haberman, A. M.; Besra, G. S.; Mohrs, M.; Brenner, M. B.; Leadbetter, E. A. Invariant Natural Killer T Cells Direct B Cell Responses to Cognate Lipid Antigen in an IL-21-Dependent Manner. *Nat. Immunol.* **2011**, *13*, 44−50.
(55) Peng, Y.; Mentzer, A. J.; Liu, G.; Yao, X.; Yin, Z.; Dong, D.; Dejnirattisai, W.; Rostron, T.; Supasa, P.; Liu, C.; Lopez-Camacho, C.; Slon-Campos, J.; Zhao, Y.; Stuart, D. I.; Paesen, G. C.; Grimes, J. M.; Antson, A. A.; Bayfield, O. W.; Hawkins, D.; Ker, D. S.; Wang, B.; Turtle, L.; Subramaniam, K.; Thomson, P.; Zhang, P.; Dold, C.; Ratcliff, J.; Simmonds, P.; de Silva, T.; Sopp, P.; Wellington, D.; Rajapaksa, U.; Chen, Y. L.; Salio, M.; Napolitani, G.; Paes, W.; Borrow, P.; Kessler, B. M.; Fry, J. W.; Schwabe, N. F.; Semple, M. G.; Baillie, J. K.; Moore, S. C.; Openshaw, P. J. M.; Ansari, M. A.; Dunachie, S.; Barnes, E.; Frater, J.; Kerr, G.; Goulder, P.; Lockett, T.; Levin, R.; Zhang, Y.; Jing, R.; Ho, L. P. Broad and Strong Memory CD4(+) and CD8(+) T Cells Induced by SARS-CoV-2 in UK Convalescent Individuals Following COVID-19. *Nat. Immunol.* **2020**, *21*, 1336−1345.
(56) Liu, C.; Ginn, H. M.; Dejnirattisai, W.; Supasa, P.; Wang, B.; Tuekprakhon, A.; Nutalai, R.; Zhou, D.; Mentzer, A. J.; Zhao, Y.; Duyvesteyn, H. M. E.; López-Camacho, C.; Slon-Campos, J.; Walter, T. S.; Skelly, D.; Johnson, S. A.; Ritter, T. G.; Mason, C.; Costa Clemens, S. A.; Gomes Naveca, F.; Nascimento, V.; Nascimento, F.; Fernandes da Costa, C.; Resende, P. C.; Pauvolid-Correa, A.; Siqueira, M. M.; Dold, C.; Temperton, N.; Dong, T.; Pollard, A. J.; Knight, J. C.; Crook, D.; Lambe, T.; Clutterbuck, E.; Bibi, S.; Flaxman, A.; Bittaye, M.; Belij-Rammerstorfer, S.; Gilbert, S. C.; Malik, T.; Carroll, M. W.; Klenerman, P.; Barnes, E.; Dunachie, S. J.; Baillie, V.; Serafin, N.; Ditse, Z.; Da Silva, K.; Paterson, N. G.; Williams, M. A.; Hall, D. R.; Madhi, S.; Nunes, M. C.; Goulder, P.; Fry, E. E.; Mongkolsapaya, J.; Ren, J.; Stuart, D. I.; Screaton, G. R. Reduced Neutralization of SARS-CoV-2 B.1.617 by Vaccine and Convalescent Serum. *Cell* **2021**, *184*, 4220−4236.
(57) Chen, X.; Chen, Z.; Azman, A. S.; Sun, R.; Lu, W.; Zheng, N.; Zhou, J.; Wu, Q.; Deng, X.; Zhao, Z.; Chen, X.; Ge, S.; Yang, J.; Leung, D. T.; Yu, H. Neutralizing Antibodies against SARS-CoV-2 Variants Induced by Natural Infection or Vaccination: A Systematic Review and Pooled Meta-Analysis. *Clin. Infect. Dis.* **2021**.
(58) Tada, T.; Zhou, H.; Dcosta, B. M.; Samanovic, M. I.; Mulligan, M. J.; Landau, N. R. Partial Resistance of SARS-CoV-2 Delta Variants to Vaccine-Elicited Antibodies and Convalescent Sera. *iScience* **2021**, *24*, 103341.
(59) Cameroni, E.; Bowen, J. E.; Rosen, L. E.; Saliba, C.; Zepeda, S. K.; Culap, K.; Pinto, D.; VanBlargan, L. A.; De Marco, A.; di Iulio, J.; Zatta, F.; Kaiser, H.; Noack, J.; Farhat, N.; Czudnochowski, N.; Havenar-Daughton, C.; Sprouse, K. R.; Dillen, J. R.; Powell, A. E.; Chen, A.; Maher, C.; Yin, L.; Sun, D.; Soriaga, L.; Bassi, J.; Silacci-Fregni, C.; Gustafsson, C.; Franko, N. M.; Logue, J.; Iqbal, N. T.; Mazzitelli, I.; Geffner, J.; Grifantini, R.; Chu, H.; Gori, A.; Riva, A.; Giannini, O.; Ceschi, A.; Ferrari, P.; Cippà, P. E.; Franzetti-Pellanda, A.; Garzoni, C.; Halfmann, P. J.; Kawaoka, Y.; Hebner, C.; Purcell, L. A.; Piccoli, L.; Pizzuto, M. S.; Walls, A. C.; Diamond, M. S.; Telenti, A.; Virgin, H. W.; Lanzavecchia, A.; Snell, G.; Veesler, D.; Corti, D. Broadly neutralizing antibodies overcome SARS-CoV-2 Omicron antigenic shift. *Nature* **2021**, DOI: 10.1038/d41586-021-03825-4.
(60) Amaral, S. P.; Fernandez-Villamarin, M.; Correa, J.; Riguera, R.; Fernandez-Megia, E. Efficient Multigram Synthesis of the Repeating Unit of Gallic Acid-Triethylene Glycol Dendrimers. *Org. Lett.* **2011**, *13*, 4522−4525.
(61) Gai, J.; Ma, L.; Li, G.; Zhu, M.; Qiao, P.; Li, X.; Zhang, H.; Zhang, Y.; Chen, Y.; Ji, W.; Zhang, H.; Cao, H.; Li, X.; Gong, R.; Wan, Y. A Potent Neutralizing Nanobody against SARS-CoV-2 with Inhaled Delivery Potential. *MedComm* **2021**, *2*, 101−113.

https://doi.org/10.1021/acs.jmedchem.1c02000
J. Med. Chem. XXXX, XXX, XXX−XXX